(12)

AFWAL-TR-82-4025

AN EMPIRICAL MODEL FOR LOAD RATIO AND TEST TEMPERATURE EFFECTS ON THE FATIGUE CRACK GROWTH RATE OF ALUMINUM ALLOY 2024-T351

Russell R. Cervay
University of Dayton
Research Institute
300 College Park Avenue
Dayton, Ohio 45469

APRIL 1982

Interim Report for Period: January - December 1981

Approved for public release; distribution unlimited.

MATERIALS LABORATORY
AIR FORCE WRIGHT AERONAUTICAL LABORATORIES
AIR FORCE SYSTEMS COMMAND
WRIGHT-PATTERSON AIR FORCE BASE, OHIO 45433

NOTICE

This technical report has been reviewed and is approved for publication.

David C Watson
DAVID C. WATSON,
Engineering and Design Data
Materials Integrity Branch

Clayton Harmsworth
CLAYTON HARMSWORTH,
Technical Manager
Engineering and Design Data
Materials Integrity Branch

FOR THE COMMANDER:

T D Cooper
T. D. COOPER, Chief
Materials Integrity Branch
Materials Laboratory

UNCLASSIFIED

SECURITY CLASSIFICATION OF THIS PAGE (When Data Entered)

REPORT DOCUMENTATION PAGE		READ INSTRUCTIONS BEFORE COMPLETING FORM
1. REPORT NUMBER AFWAL-TR-82-4025	2. GOVT ACCESSION NO. AD-A116 567	3. RECIPIENT'S CATALOG NUMBER
4. TITLE (and Subtitle) AN EMPIRICAL MODEL FOR LOAD RATIO AND TEST TEMPERATURE EFFECTS ON THE FATIGUE CRACK GROWTH RATE OF ALUMINUM ALLOY 2024-T351		5. TYPE OF REPORT & PERIOD COVERED Interim Technical Report January-December 1981
		6. PERFORMING ORG. REPORT NUMBER UDR-TR-82-42
7. AUTHOR(s) Russell R. Cervay		8. CONTRACT OR GRANT NUMBER(s) F33615-80-C-5011
9. PERFORMING ORGANIZATION NAME AND ADDRESS University of Dayton Research Institute 300 College Park Avenue Dayton, Ohio 45469		10. PROGRAM ELEMENT, PROJECT, TASK AREA & WORK UNIT NUMBERS 2421-03-15
11. CONTROLLING OFFICE NAME AND ADDRESS Air Force Wright Aeronautical Laboratories Materials Laboratory (AFWAL/MLSA) Wright-Patterson AFB, Ohio 45433		12. REPORT DATE April 1982
		13. NUMBER OF PAGES 50
14. MONITORING AGENCY NAME & ADDRESS(if different from Controlling Office)		15. SECURITY CLASS. (of this report) Unclassified
		15a. DECLASSIFICATION/DOWNGRADING SCHEDULE

16. DISTRIBUTION STATEMENT (of this Report)

Approved for public release; distribution unlimited.

17. DISTRIBUTION STATEMENT (of the abstract entered in Block 20, if different from Report)

18. SUPPLEMENTARY NOTES

19. KEY WORDS (Continue on reverse side if necessary and identify by block number)

Aluminum
2024-T351
Fatigue Crack Growth
Mathematical Modeling
Load Ratio
R-ratio
Elevated Temperature

20. ABSTRACT (Continue on reverse side if necessary and identify by block number)

Constant amplitude loading fatigue crack growth rate test data were generated for aluminum alloy 2024-T351 at 20 test conditions: the combination of five load ratios, 0.01, 0.1, 0.3, 0.5, and 0.6 and four test temperatures, 72°, 200°, 300°, and 400°F (22°, 93°, 149°, and 204°C, respectively). A mathematical model of the shift in the linear data region with the variation in test temperature and/or load ratio was formulated. The model

DD FORM 1473 1 JAN 73 EDITION OF 1 NOV 65 IS OBSOLETE

UNCLASSIFIED

SECURITY CLASSIFICATION OF THIS PAGE (When Data Entered)

20. Abstract (Concluded)

approximates the log-Paris coefficient as a linear relationship of both the R-ratio and test temperature assuming all other test parameters remain constant.

Using the model a predictive equation was formulated for an unexplored test condition, R=0.35 and a 250°F (121°C), prior to the generation of test data at that test-case test condition. Following the generation of data at the test-case load ratio/ test temperature, the best fitting equation to the linear region of the test-case data set was then calculated; this best fitting equation was found to agree very well with the predictive equation formulated beforehand.

PREFACE

This interim technical report was submitted by the University of Dayton Research Institute, Dayton, Ohio, under Contract F33615-80-C-5011, "Quick Reaction Evaluation of Materials," with the Materials Laboratory of the Air Force Wright Aeronautical Laboratories, Wright-Patterson Air Force Base, Ohio.

This effort was conducted during the period of January 1981 through December 1981. The author, Mr. Russell R. Cervay, would like to extend special recognition to Mr. Donald W. Woleslagle and Mr. Richard Marton of the University of Dayton for the painstaking care and diligent attention they demonstrated in generating the fatigue crack growth test data presented herein.

This report was submitted by the author in March 1982.

TABLE OF CONTENTS

LIST OF ILLUSTRATIONS

LIST OF ILLUSTRATIONS (Concluded)

LIST OF TABLES

SECTION I
INTRODUCTION

A simple empirically based mathematical model for constant amplitude loading fatigue crack growth rate (FCGR) test data is very useful for predicting the crack growth rate for a particular material at a condition where test data are non-existent. In this manner the necessity for generating data at a particular unexamined test condition is circumvented. There are several models already in existence that vary in their degree of complexity and their degree of success in predicting test data results. Reference 1 discusses a simple empirical model for the shift in the linear region of room temperature FCGR data for aluminum alloy 7010-T73651 with a change in load ratio, R-ratio (minimum load/maximum load). The linear data region of FCGR test data is depicted in Figure 1. The model was based on the Paris equation:

$$da/dn = C\Delta K^{m} \tag{1}$$

where da/dn is the crack extension per load cycle, termed the fatigue crack growth rate, ΔK is the stress intensity range, and C and m are material dependent constants. The Paris equation is applicable to the linear data region only (assuming the log-stress intensity range, log-ΔK, is plotted versus the log-crack growth rate); the threshold and rapid growth rate regions are not considered in this expression (Figure 1). The Reference 1 model represents the log-Paris coefficient, log-C, as linearly related to the changing R-ratio at room temperature, assuming a fixed exponent. See Figure 2 . The model was successful at accurately predicting the best fit straight line to the linear data region prior to the generation of the data.

This program expands the model developed in Reference 1 to account for variation of the test temperature. To accomplish this, three issues will be addressed. At elevated temperatures does there still exist a linear relationship

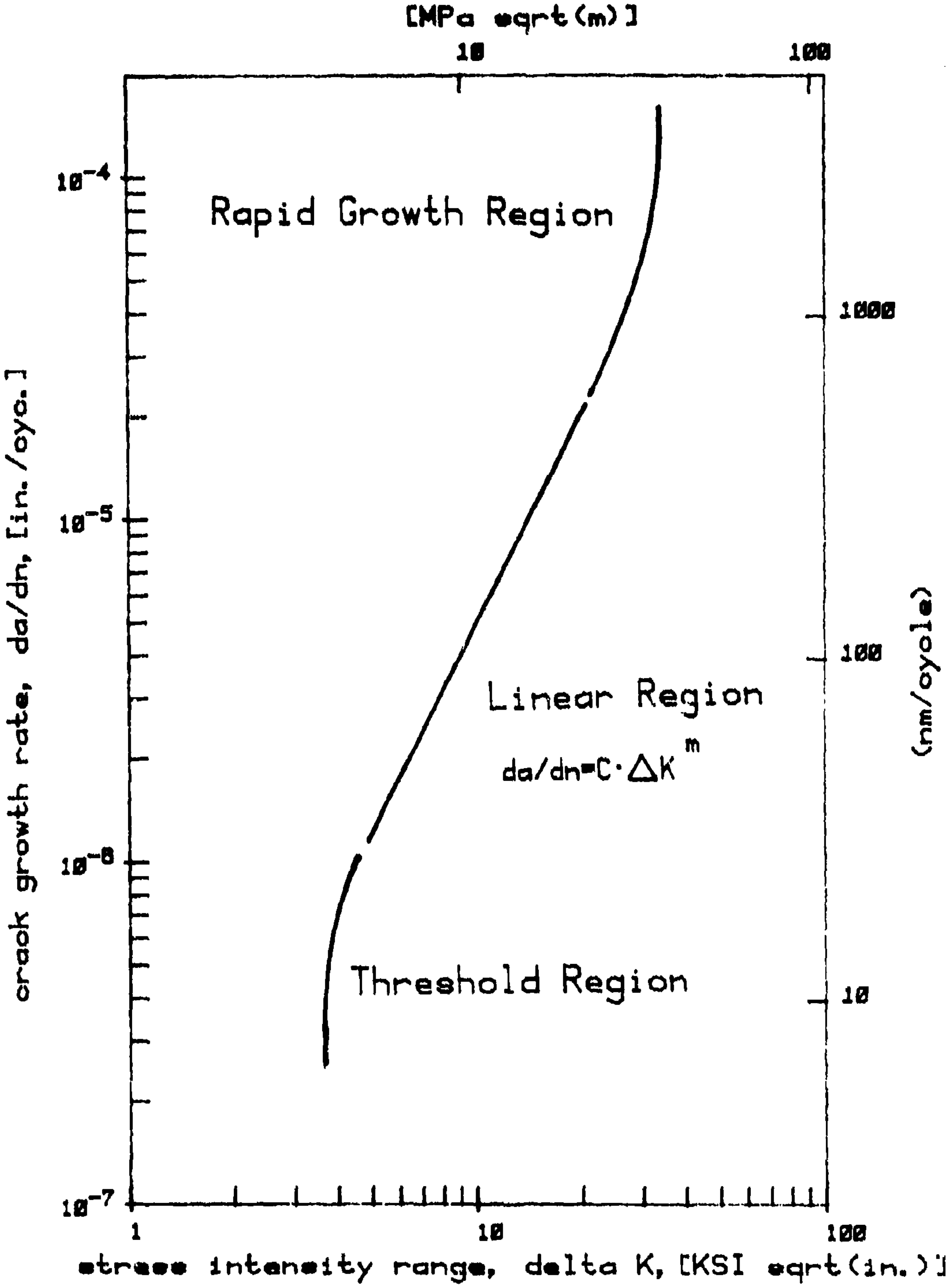

Figure 1. Conventional Presentation of Constant Amplitude Loading FCGR Test Data.

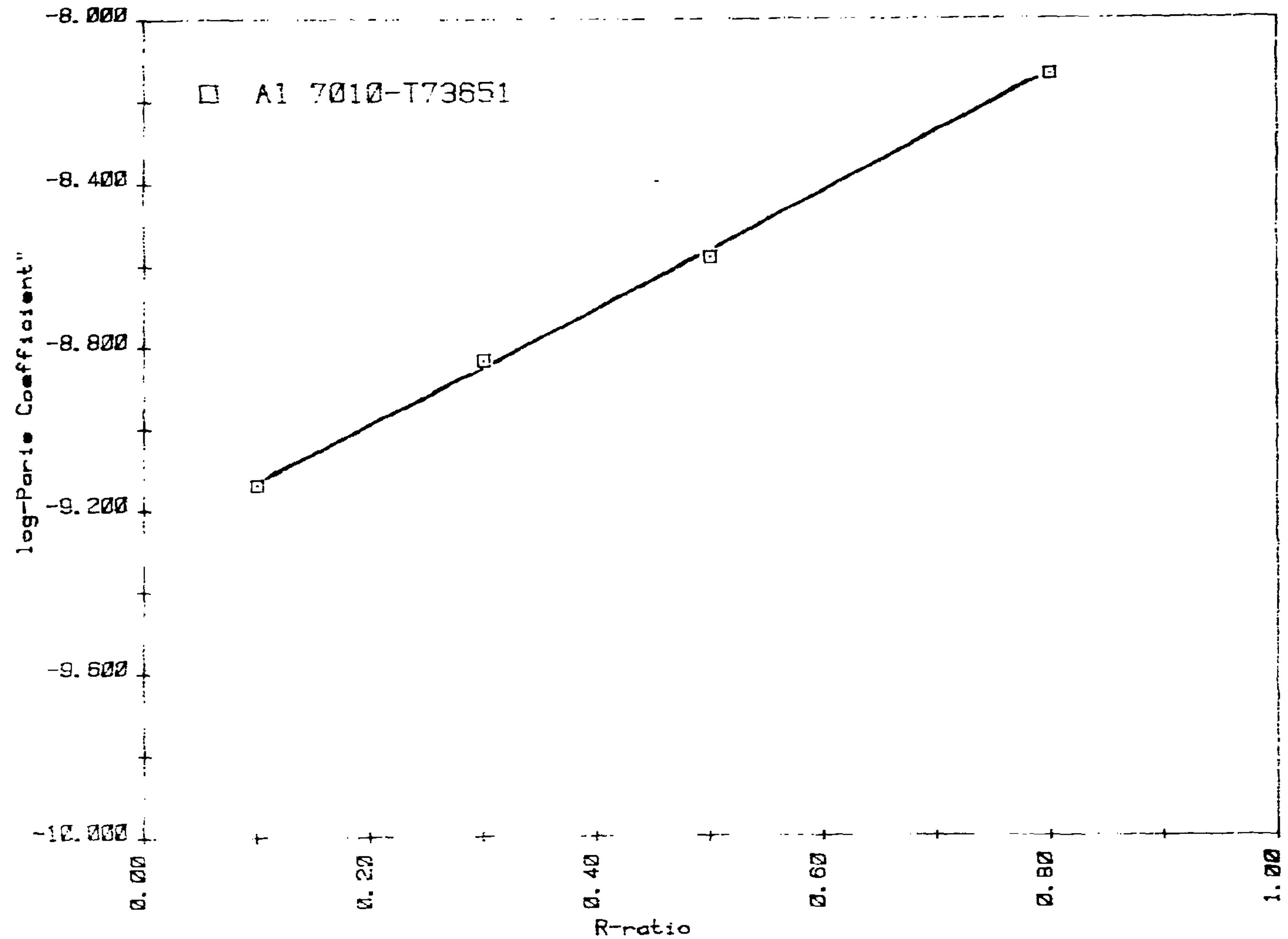

Figure 2. Log-Paris Coefficient Versus R-Ratio for Aluminum Alloy 7010-T73651.

between the R-ratio and the log-Paris coefficient? If so, is there a trend in the lines' slopes with a change in test temperature? Lastly, with the R-ratio held constant can a simple mathematical relationship be defined to accommodate the shift in the data's linear region with a change in test temperature?

SECTION II
TEST PROGRAM AND SPECIMENS

The test material was aluminum alloy 2024, half inch (12.7 mm) thick, bare, rolled plate. It was produced by the Aluminum Company of America. The material was provided in the T351 condition which is a solution heat treatment followed by cold working and natural aging. The results of a chemical constituent analysis is presented as follows.

Chemical Constituent Composition

Cu	Mg	Mn	Fe	Si	Ti	Al
4.3	1.5	0.58	0.20	0.16	<0.03	Balance

Tensile specimens were machined from the test plate and triplicate tensile tests were performed at the four test temperature of interest: 72°, 200°, 300°, and 400°F (22°, 93°, 149°, and 204°C, respectively). The specimens were machined in accord with Figure 3. All tensile specimens were fabricated with the loading direction parallel to the plate's longitudinal grain direction. All of these tests were conducted in compliance with the applicable ASTM test standard, E-8, "Tensile Testing of Metallic Materials."

Two to six constant amplitude loading FCGR tests were completed at each of 20 different test conditions. The test conditions were the combination of five different R-ratios: 0.01, 0.1, 0.3, 0.5, and 0.6, and the four different test temperatures: 72°, 200°, 300°, and 400°F (22°, 93°, 149°, and 204°C, respectively). All of the FCGR tests were conducted in accord with ASTM test procedure E647-78, "Constant-Load-Amplitude Fatigue Crack Growth Rates Above 10^{-8} m/cycle." Also, all of these FCGR tests: (1) were conducted in a laboratory air environment, (2) used a loading frequency equal to 20 Hz, and (3) used the CT specimen shown in Figure 4 with L-T grain orientation.

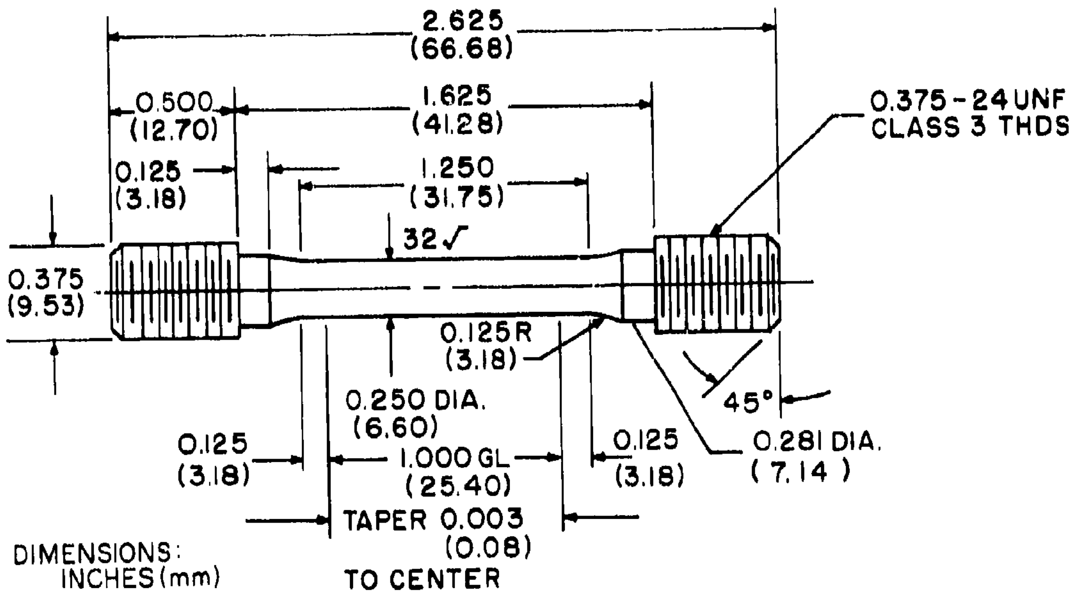

Figure 3. Tensile Test Specimen.

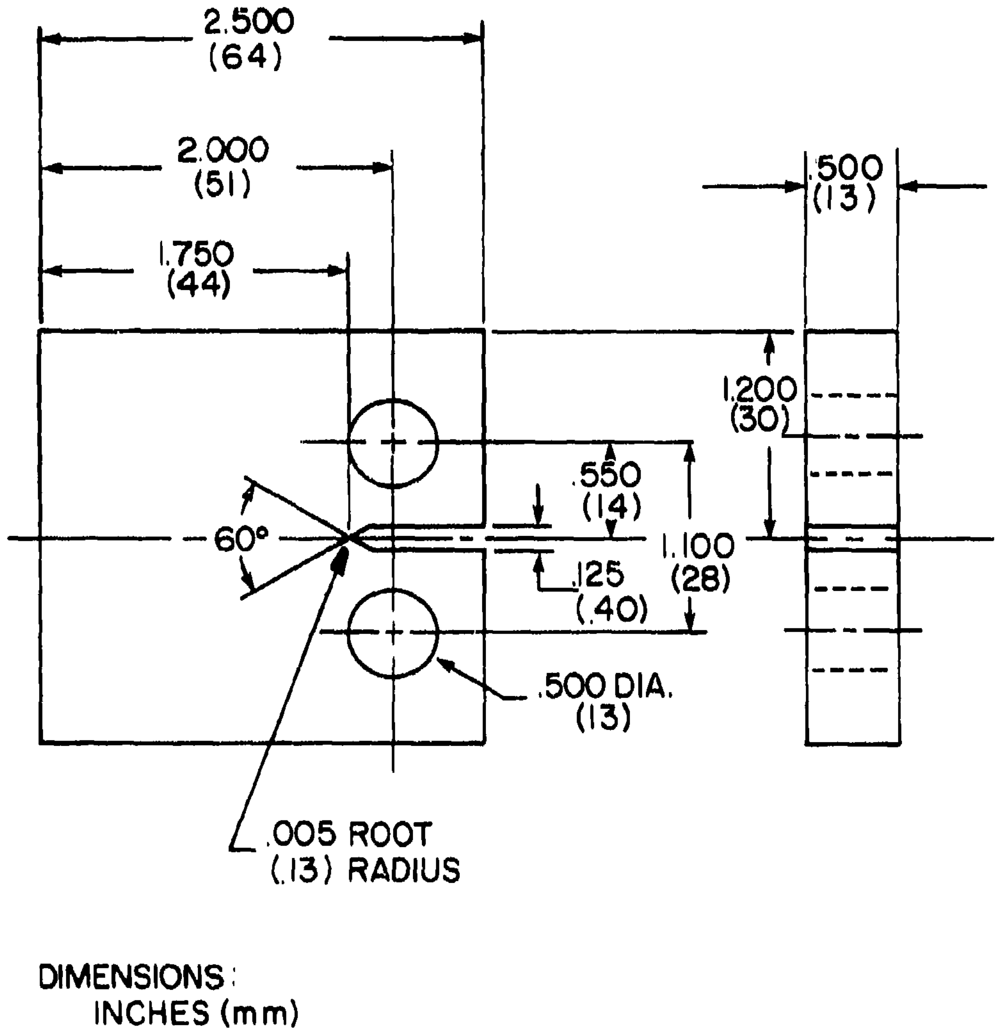

Figure 4. CT Fatigue Crack Growth Test Specimen.

Only the linear region of the crack growth rate data as represented on a log-stress intensity range versus log-crack growth rate pair of axes was considered in this effort; the threshold and rapid crack growth rate region immediately preceding failure were not considered and are not presented herein. The maximum and minimum crack growth rates that were used to define the linear region for each of the 20 test conditions are listed in Table 1; these limits represent conservative subjective judgements; generally, the linear region extends beyond these limits.

For the first 23 tests completed, which represent each R-ratio in combination with either a 72°F (22°C) or 200°F (93°C) test temperature, the Paris exponent and coefficient were allowed to freely vary when calculating the best fitting linear equation to these individual specimen's data sets. The average value exponent of these 23 individual specimen data sets was 3.36 with the maximum value of 3.50 and a minimum value of 3.27 or a range of plus or minus 4 percent. Subsequently in calculating the best fitting equation to the 20 multi-specimen data sets the Paris exponent was fixed equal to $\overline{m}=3.36$, and only the Paris coefficient, C, was allowed to freely vary.

Following the calculation of the best fitting equation to each of the 20 data sets in accord with the above described procedure a mathematical model of the shift in the Paris coefficient for a change in R-ratio and/or test temperature was formulated. The formulated mathematical model was used to predict the best fitting equation to a test case set of data prior to the generation of the test case data. The test case was arbitrarily selected to be 250°F (121°C) at a load ratio of 0.35.

TABLE 1

MAXIMUM AND MINIMUM CRACK GROWTH RATES INCLUDED
AS LINEAR DATA REGION

da/dn - in/cycle (nm/cycle)

Test Temp. °F(°C)	R= 0.01	0.1	0.3	0.5	0.6
72(22)	7.0×10^{-5}(1778)	7.0×10^{-5}(1778)	6.5×10^{-5}(1651)	4.0×10^{-5}(1016)	2.0×10^{-5}(508)
	2.0×10^{-6}(51)	2.0×10^{-6}(51)	2.0×10^{-6}(51)	2.0×10^{-6}(51)	2.0×10^{-6}(51)
200(93)	7.0×10^{-5}(1788)	7.0×10^{-5}(1778)	6.5×10^{-7}(1651)	4.0×10^{-5}(1016)	2.0×10^{-5}(508)
	2.0×10^{-6}(51)	2.0×10^{-6}(51)	1.5×10^{-6}(38)	1.5×10^{-6}(38)	1.5×10^{-6}(38)
300(149)	7.0×10^{-5}(1778)	7.0×10^{-5}(1778)	6.5×10^{-7}(1651)	4.0×10^{-5}(1016)	2.0×10^{-5}(508)
	2.0×10^{-6}(51)	2.0×10^{-6}(51)	1.5×10^{-6}(38)	1.5×10^{-6}(38)	1.5×10^{-6}(38)
400(204)	7.0×10^{-5}(1778)	7.0×10^{-5}(1778)	6.5×10^{-7}(1651)	4.0×10^{-5}(1016)	1.0×10^{-5}(254)
	2.0×10^{-6}(51)	2.0×10^{-6}(51)	1.5×10^{-6}(38)	1.5×10^{-6}(38)	8.0×10^{-7}(20)

SECTION III
RESULTS AND DISCUSSION

Tensile test results are presented in Table 2. The material is a moderate strength and ductile aluminum alloy/ heat treatment. For the temperature rise from room temperature to 400°F (204°C) the average ultimate strength decreases 27.0 percent, whereas, the average yield strength only decreases 10.5 percent. For the same temperature rise there is little change in the percent elongation at failure, however, there is a large increase in the percent reduction of area.

The linear region FCGR test results are presented in Appendix A in Figures A.1 through A.20. Generally, the linear region shifts down and to the left with an increase in R-ratio and for this material changes very little with an increase in temperature. The best fitting equation that was calculated for each data set with the exponent fixed equal to $\bar{m}$=3.36 is also listed on each of the 20 figures. From this point on in the discussion of modeling the FCGR data with the Paris equation, the stress intensity range, ΔK, is in KSI$\sqrt{\text{in}}$, the crack growth rate, da/dn, is in in./cycle and the temperature is in degrees Fahrenheit (°F).

Table 3 lists the logarithm of the Paris coefficient, log-C, for all 20 test conditions of interest. Figure 5 presents a plot of the loading ratio versus the log-Paris coefficient. Here if the points for a load ratio equal to 0.01 are excluded the load ratio versus log-Paris coefficient can fairly well be represented as a straight line, as was done in Reference 1. This is true not only of the room temperature tests but is equally applicable to the elevated temperature data. The lowest load ratio Paris coefficients do not coordinate well with the coefficient associated with larger R-ratios. Similarly, in Reference 1 the Paris coefficient of some data for load ratios less than or equal to zero was not linearly related to those coefficients for the same material generated at higher R-ratios.

TABLE 2

ALUMINUM ALLOY 2024-T351 TENSILE TEST RESULTS

Test Temperature °F	(°C)	Ultimate Strength KSI (MPa)	0.2% Yield Strength KSI (MPa)	Elongation in 0.5 in. (12.7 mm) G.L. (%)	Reduction of Area (%)
72	(22)	66.1(455.7)	50.4(347.5)	27.6	24.8
		66.2(456.4)	50.8(350.3)	26.3	21.7
		65.3(450.2)	53.2(366.8)	23.6	25.5
	Avg.	65.9(454.1)	51.5(354.9)	25.8	24.0
200	(93)	62.2(428.9)	49.4(340.6)	23.3	26.1
		62.4(430.2)	49.1(338.5)	26.8	28.7
		62.9(433.7)	49.3(339.9)	26.7	25.7
	Avg.	62.5(430.9)	49.3(339.7)	25.6	26.8
300	(149)	56.1(386.8)	45.9(316.5)	27.0	31.8
		55.7(384.0)	47.5(327.5)	30.0	34.8
		56.9(392.3)	46.3(319.2)	29.3	33.0
	Avg.	56.2(387.7)	46.6(321.1)	28.8	33.2
400	(204)	47.5(327.5)	45.8(315.8)	22.1	42.0
		47.7(328.9)	45.7(315.1)	23.8	43.0
		49.2(339.2)	46.7(322.0)	23.0	44.0
	Avg.	48.1(331.9)	46.1(317.6)	23.0	43.0

TABLE 3

LOG-PARIS COEFFICIENT FOR Al2024-T351

Test Temperature °F	(°C)	R= 0.01	0.1	0.3	0.5	0.6
72	(22)	-8.613	-8.447	-8.350	-8.277	-8.231
200	(93)	-8.565	-8.409	-8.336	-8.257	-8.212
300	(149)	-8.500	-8.402	-8.323	-8.257	-8.178
400	(204)	-8.513	-8.356	-8.275	-8.205	-8.145

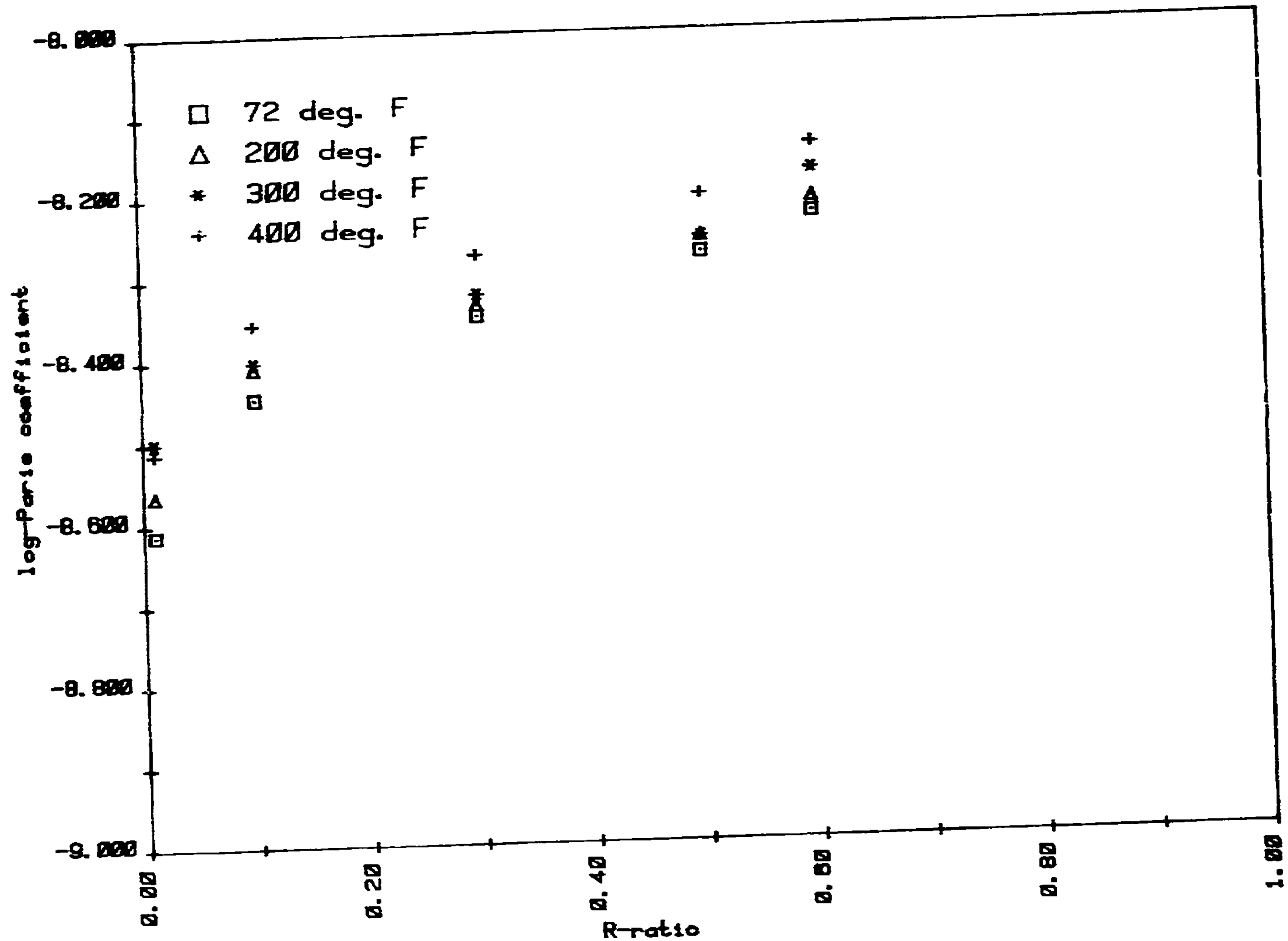

Figure 5. Loading Ratio Versus Log-Paris Coefficient.

In general, there is very little shift in the data points in going from the 72°F (22°C) to the 400°F (204°C) data. This is a very desirable material characteristic but presents a hurdle in this effort to characterize a material's response to a change in temperature.

In Figure 5 if lines were drawn through the data points for each temperature, excluding all of the log-Paris coefficients for an R-ratio equal to 0.01, the slopes of the four lines (not shown) would be 0.417, 0.392, 0.424, and 0.418 for the four test temperatures: 72°F (22°C), 200°F (93°C), 300°F (149°C), and 400°F (204°C), respectively. Since (1) there is no trend in the slopes, and (2) the slope for 72°F (22°C) and 400°F (204°C), the minimum and maximum test temperatures, are practically identical, the slope was assumed to be constant over the temperature range and is approximately equal to the average of the four values $\bar{b} = 0.413$. Assuming the slope of the line remains constant will accommodate considerable simplification of the mathematical model for the FCGR test data since

$$\text{log-C} \approx \text{constant} + \bar{b} \cdot R$$

is equally applicable for any temperature. Also the Paris exponent, m, is assumed to be constant, $\bar{m}=3.36$, over the entire R-ratio, temperature, and crack growth rate range (Table 1) included in this program, which represents another convenient simplification.

Figure 6 presents the log-Paris coefficients listed in Table 3 along with the temperatures. For all five R-ratios there is very little change in crack growth data (Figures A.4 to A.20) or in log-C with an increase in temperature. Here again it can be seen that all of the log-C values associated with a loading ratio equal to 0.01 plot disproportionately low.

A linear relationship can quite adequately represent the change in log-C with test temperature for all five of the R-ratios.

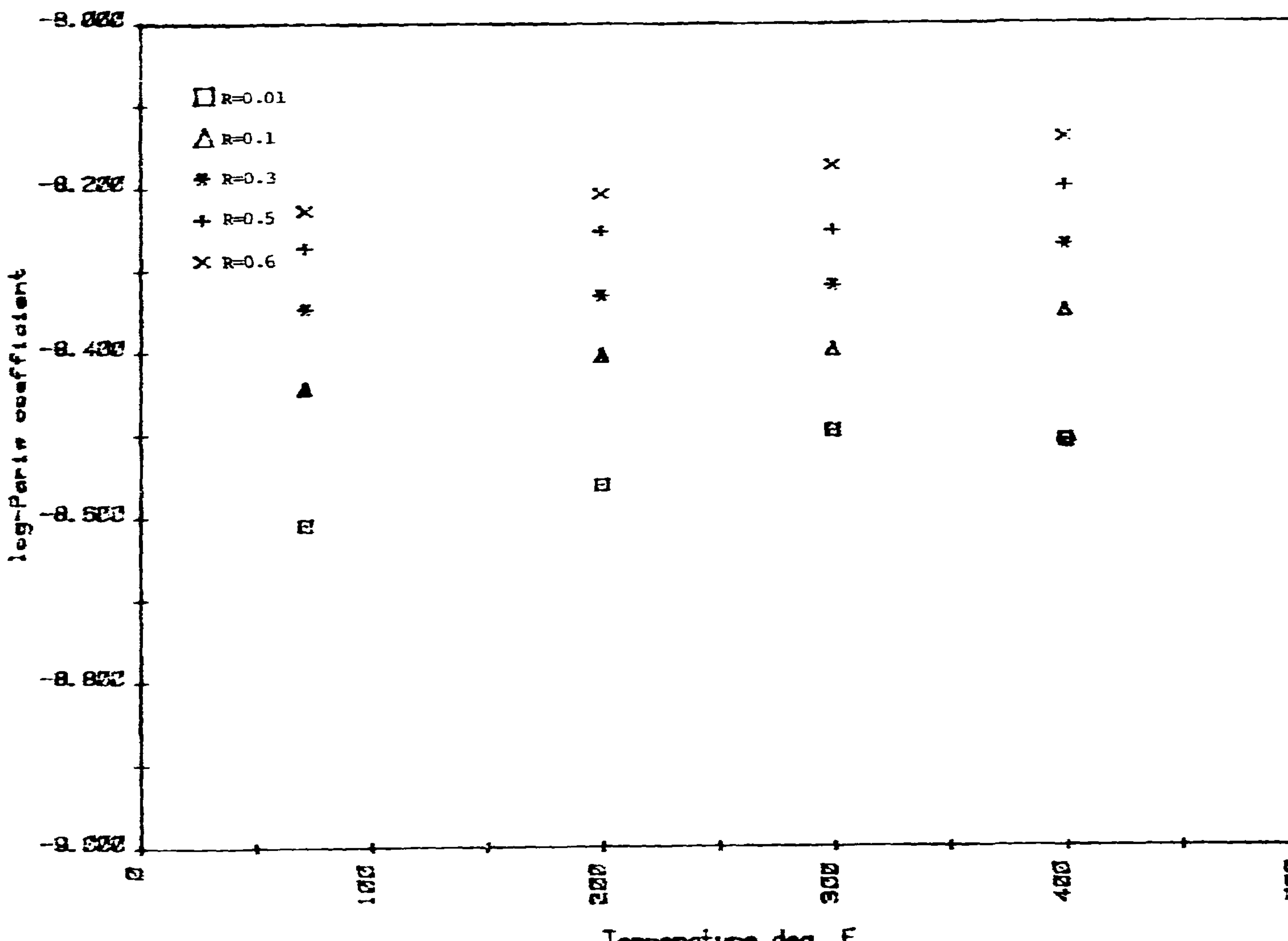

Figure 6. Test Temperature Versus Log-Paris Coefficient.

If the best fit lines (not shown) were drawn for each R-ratio, the slope of each line would be: 0.00031, 0.00026, 0.00021, 0.00019, and 0.00027 for loading ratios equal to 0.01, 0.1, 0.3, 0.5, and 0.6, respectively (since the plot for an R-ratio equal to 0.01 is disproportionally low these log-coefficients data points will again be disregarded). The average slope for the four lines associated with the R-ratios larger than 0.01 is $\bar{d}=0.00023$. This average slope is represented as only an approximate value for the change in log-C with a change in temperature. Assuming the slope of the lines remains constant represents another convenient simplification of the mathematical model for the FCGR data. Consequently,

$$\log\text{-}C \approx \text{constant} + \bar{d}\cdot T$$

is equally applicable over the R-ratio range from 0.1 to 0.6.

It has been assumed that the trivariant data (R-ratio, test temperature, and log-C) can be graphically represented by a series of parallel straight lines. Reference 2 presents a least squares method for calculating the coefficients for trivariant linearly related data in the general form

$$z = a_0 + a_1 x + a_2 y \qquad (2)$$

for a given set of n data points where

$$a_2 = \frac{N_1 - N_2}{[n\ \Sigma x_i^2 - (\Sigma x_i)^2][n\ \Sigma y_i^2 - (\Sigma y_i^2)] - [n\ \Sigma x_i y_i - (\Sigma x_i)(\Sigma y_i)]^2} \qquad (3)$$

where

$$N_1 = [n\ \Sigma x_i^2 - (\Sigma x_i)^2][n\ \Sigma y_i z_i - (\Sigma y_i)(\Sigma z_i)] \qquad (4)$$

$$N_2 = [n\ \Sigma\text{-}x_i y_i - (\Sigma x_i)(\Sigma y_i)][n\ \Sigma x_i z_i - (\Sigma x_i)(\Sigma z_i)] \qquad (5)$$

$$a_1 = \frac{[n\ \Sigma x_i z_i - (\Sigma x_i)(\Sigma z_i)] - a_2[n\ \Sigma x_i y_i - (\Sigma x_i)(\Sigma y_i)]}{n\ \Sigma x_i^2 - (\Sigma x_i)^2} \quad (6)$$

and $$a_0 = \frac{\Sigma z_i - a_2 \Sigma y_i - a_1 \Sigma x_i}{n} \quad (7)$$

for $i = 1,2,3\ldots n$

For this particular application

x = R-ratio = R

y = Test temperature (°F) = T

and z = log-C.

Since the data for an R-ratio equal to 0.01 appears to be disproportionately low, only the 16 data points (n=16) for R-ratios greater than or equal to 0.1 were used as input to the above equations. The results of the calculations were

$a_0 = -8.503$

$a_1 = 0.412$

and $a_2 = 0.00023$

$$\text{or } \log C = -8.503 + 0.412R + 0.00023T \quad (8)$$

The two coefficients calculated in this manner are practically identical to the average values for the lines' slopes (Figures 3 and 4) presented as approximations earlier. Taking the antilogarithm of equation (8) yields a general expression for the Paris coefficient, C,

$$C = 10^{(-8.503+0.412R+0.00023T)} \quad (9)$$

Therefore, by substituting equation (9) and the average exponent, $\overline{m}$=3.36, into equation (1) the final mathematical model for the test material is:

$$\frac{da}{dn} = 10^{(-8.503+0.412R+0.00023T)} \Delta K^{3.36} \quad (10)$$

for $72° \leq T \leq 400°F$ and $0.1 \leq R \leq 0.6$.

A test case to verify the general Paris expression (10) was arbitrarily selected at an R-ratio equal to 0.35 and a test temperature of 250°F (121°C). Putting the values of these two parameters into equation (10) a predictive equation for the data is obtained:

$$\frac{da}{dn} = 10^{(-8.503+0.412\cdot 0.35+0.00023\cdot 250)} \Delta K^{3.36}$$

$$\frac{da}{dn} = 10^{(-8.302)} \Delta K^{3.36} \qquad (11)$$

$$\frac{da}{dn} = 4.99 \cdot 10^{-9} \Delta K^{3.36} \text{ for R=0.35 and T=250°F (121°C)}$$

Two specimens were tested for the test case. Test results are presented in Figure 7 along with the best fitting line calculated with the exponent fixed equal to 3.36. (The best fitting equation calculated for this same data set with both the exponent and coefficient free to vary has the same exponent, 3.36, and a coefficient equal to $4.76\cdot 10^{-9}$ rather than $4.75\cdot 10^{-9}$.) Also presented in Figure 7 is the predictive equation (11). The two lines overlap. They were started and ended at different stress intensity ranges to facilitate visual detection of two different lines as opposed to one broad line. Agreement between the predictive and best fitting equation for the test case data set is excellent.

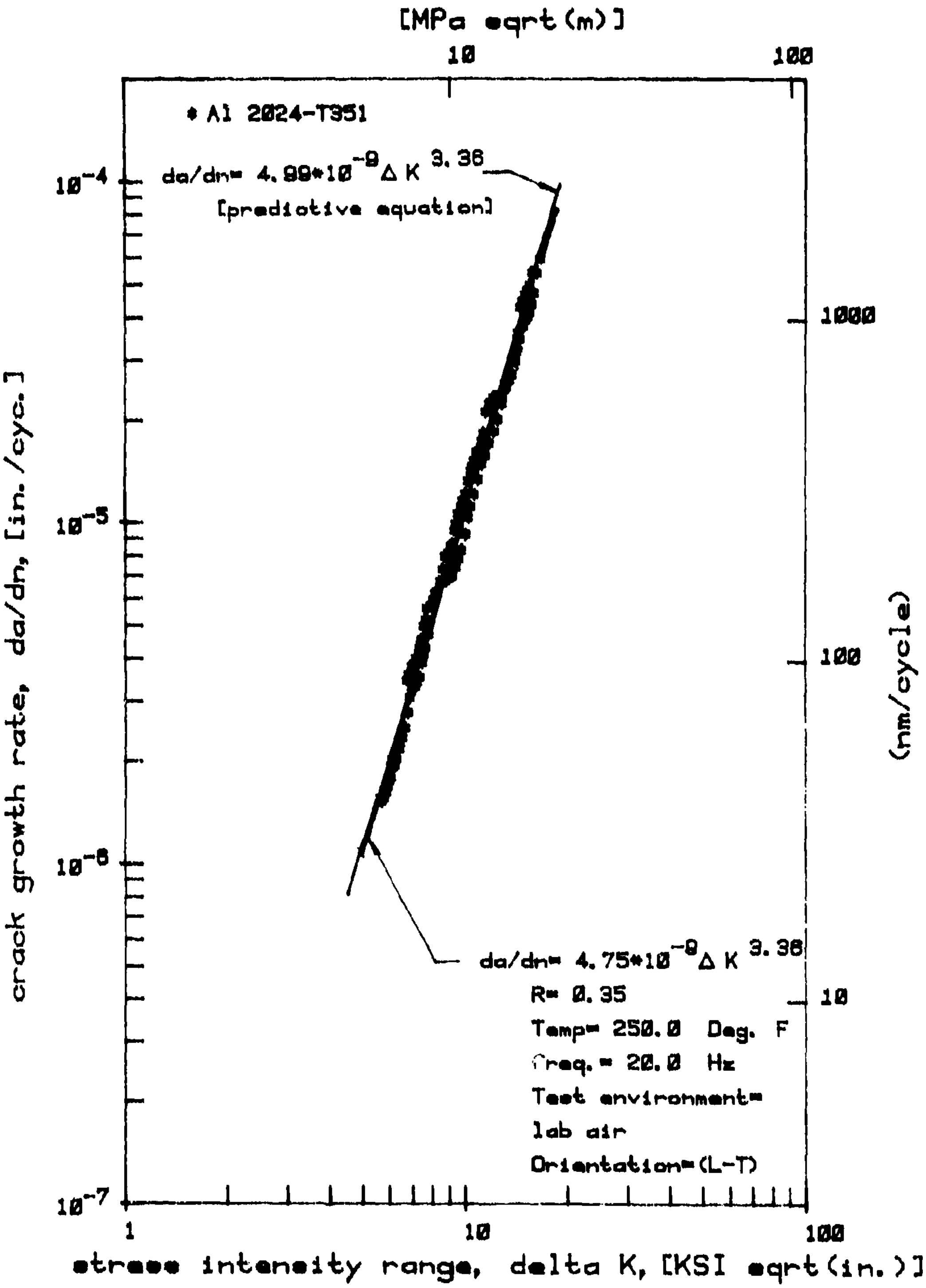

Figure 7. R=0.35, 250°F (121°C) FCGR Test Results.

SECTION IV
CONCLUSIONS

The following conclusions are applicable for the test conditions used throughout this report; i.e., 72°F (22°C) $\leq$ Temperature $\leq$ 400°F (204°C), 0.1 $\leq$ R-ratio $\leq$ 0.6, and a loading frequency equal to 20 Hz.

1. The log-Paris coefficient can be modeled as a linear relationship of the R-ratio and the test temperature assuming all other test parameters remain constant.
2. In a log-stress intensity range versus the log-crack growth rate plot the linear region shifts down and to the left with increasing R-ratio.
3. For a constant loading frequency and load ratio there is very little acceleration in the crack growth rate in aluminum alloy 2024-T351 with an increase in test temperature.
4. The crack growth model derived herein netted a good fitting predictive equation to the linear region of a test case data set.

REFERENCES

1. Cervay, Russell R., "An Empirical Model for Loading Ratio Effect on Fatigue Crack Growth Rate Data," University of Dayton Research Institute, Technical Report AFWAL-TR-81-4140, November 1981.

2. Program Manual ST1 Statistical Library, Texas Instrument Incorporated, Dallas, Texas, 1975.

APPENDIX A

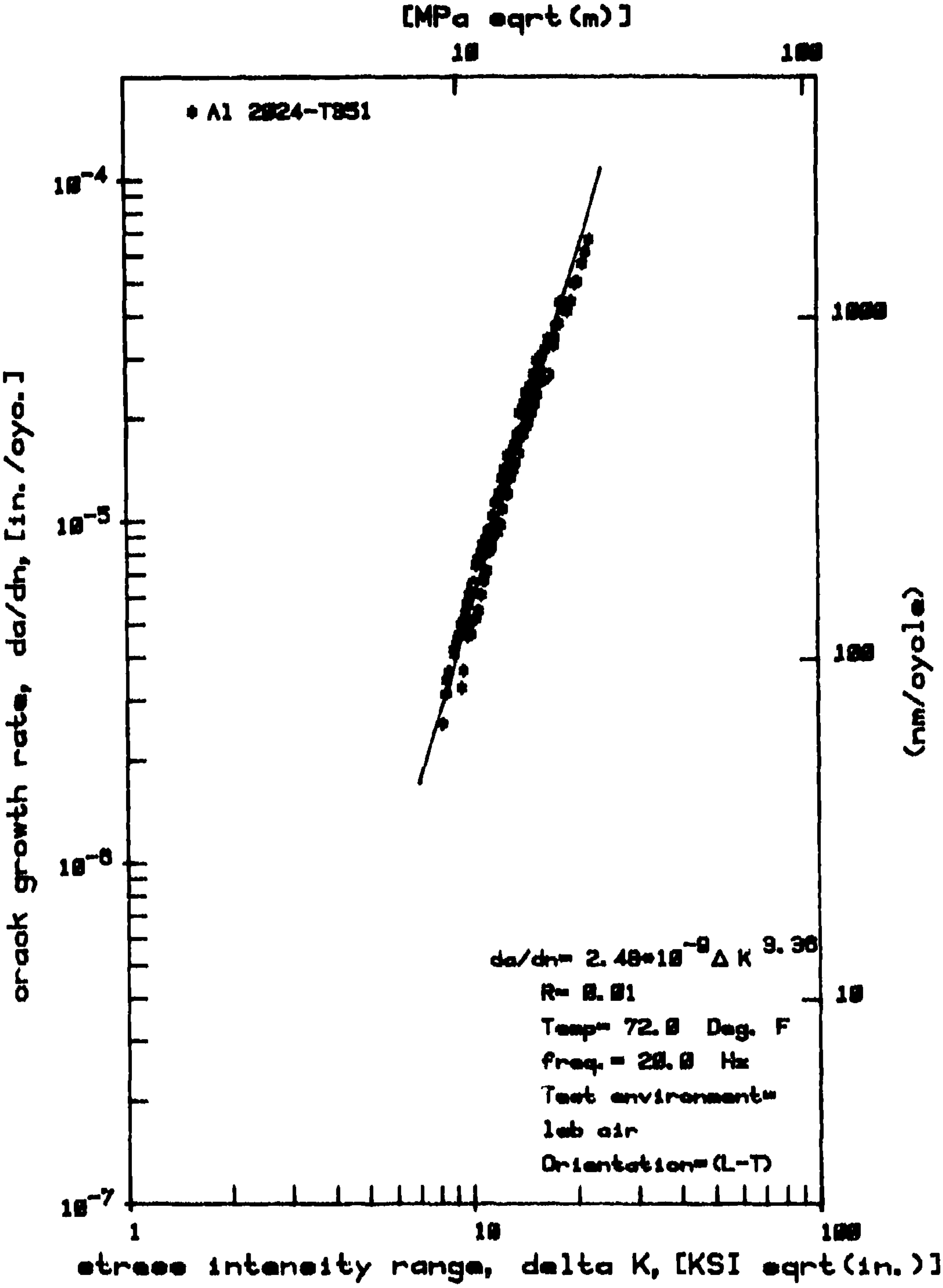

Figure A.1. R=0.01, 72°F (22°C) FCGR Test Results.

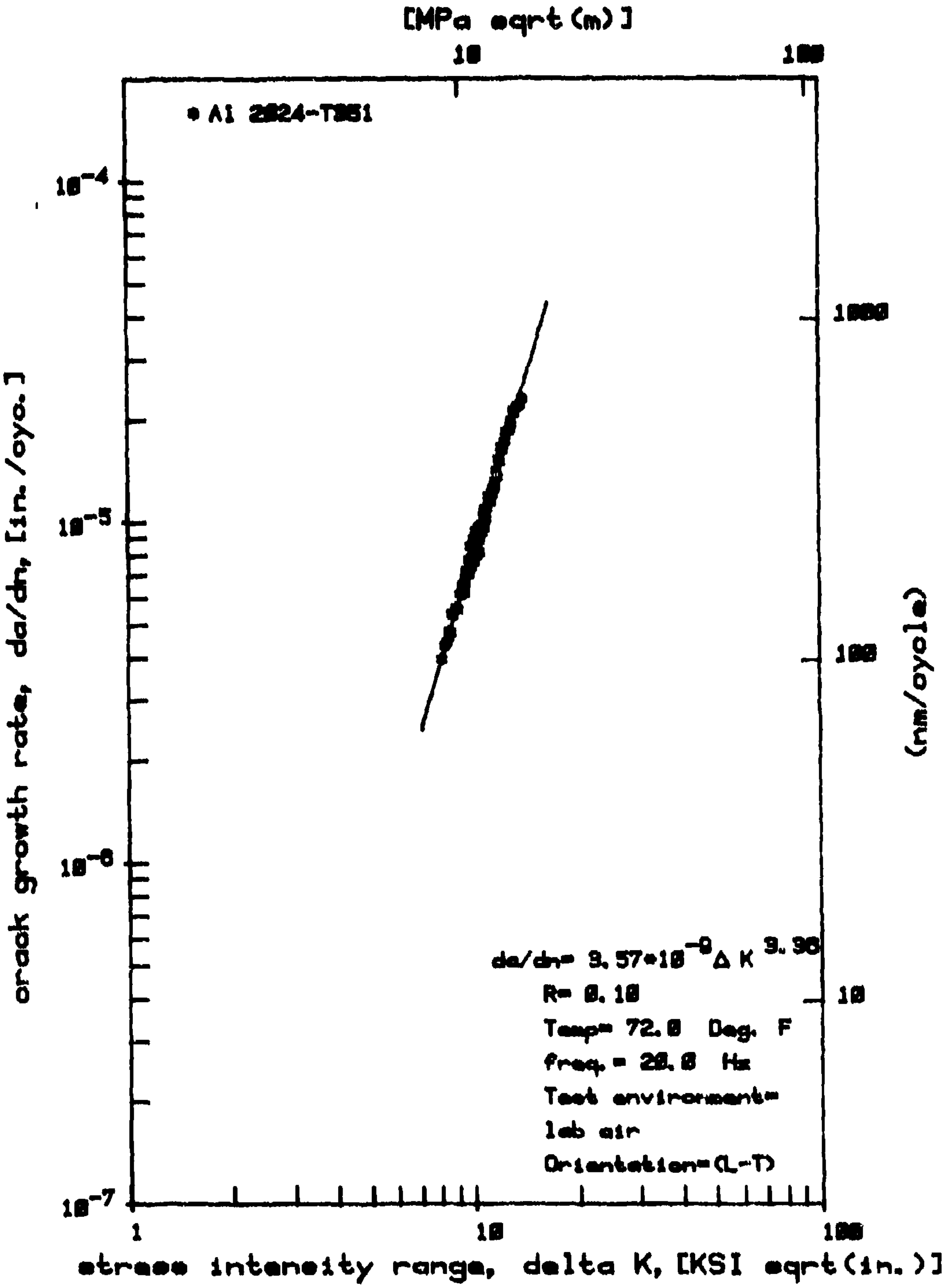

Figure A.2. R=0.1, 72°F (22°C) FCGR Test Results.

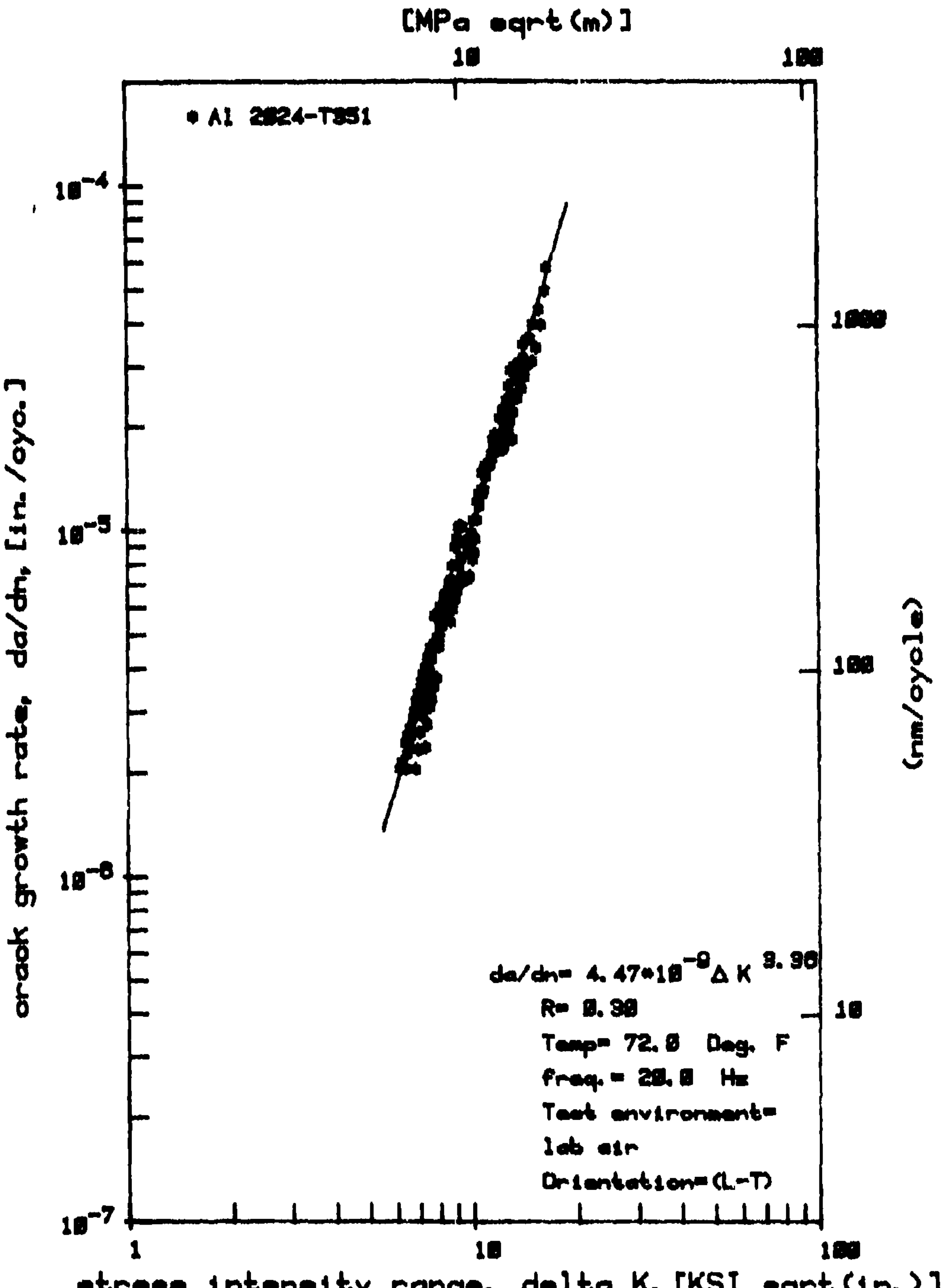

Figure A.3. R=0.3, 72°F (22°C) FCGR Test Results.

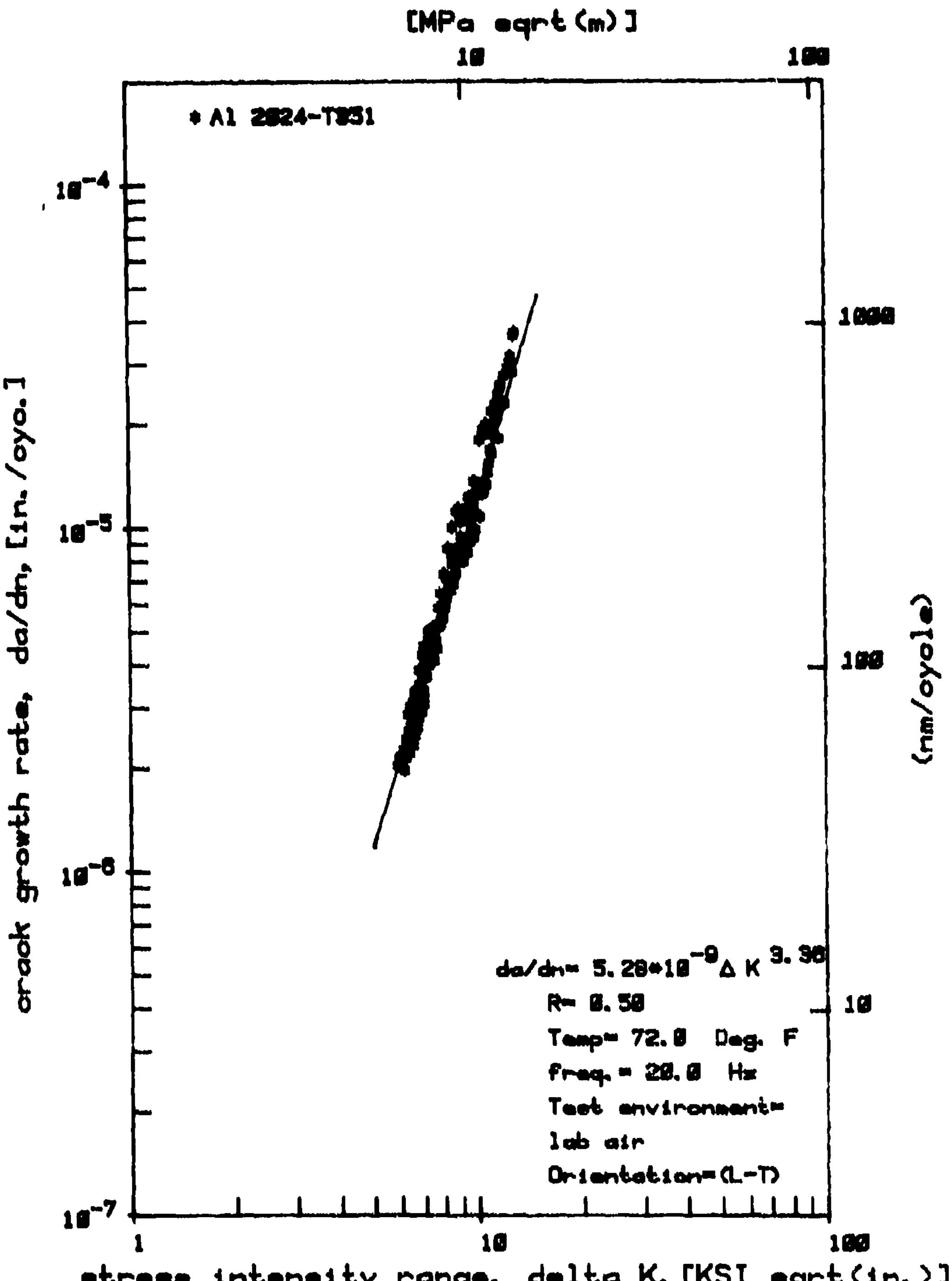

Figure A.4. R=0.5, 72°F (22°C) FCGR Test Results.

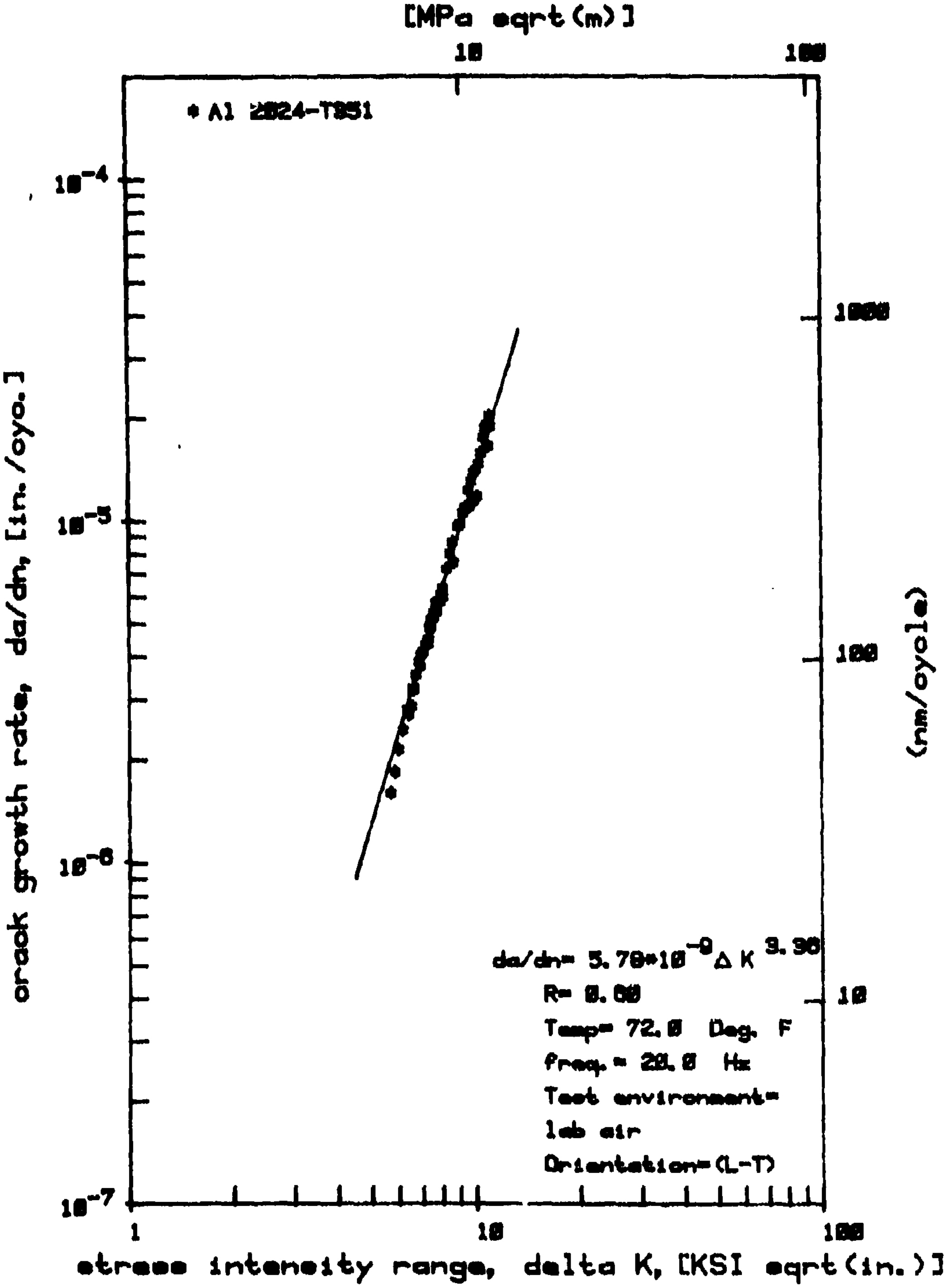

Figure A.5. R=0.6, 72°F (22°C) FCGR Test Results.

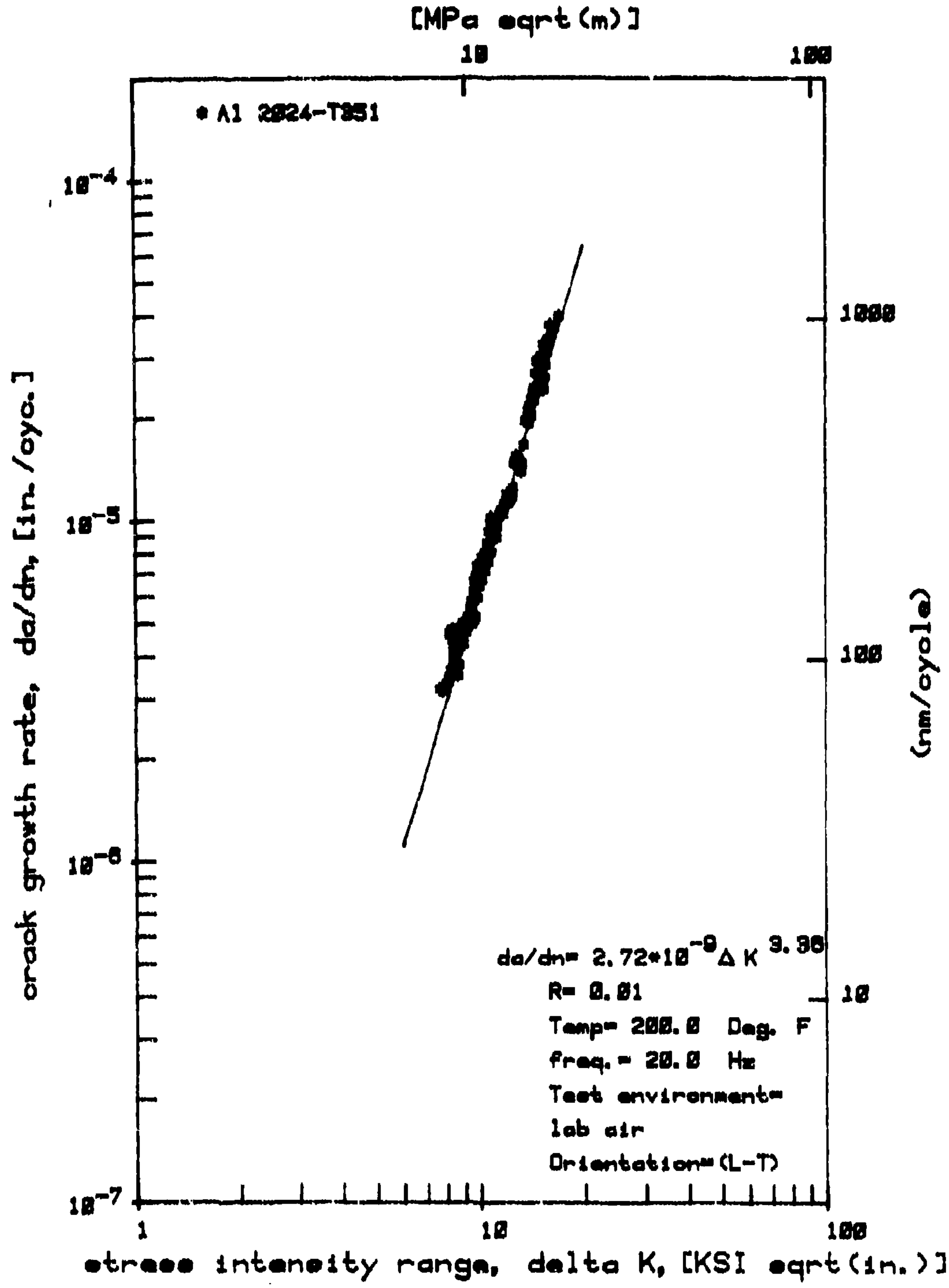

Figure A.6. R=0.01, 200°F (93°C) FCGR Test Results.

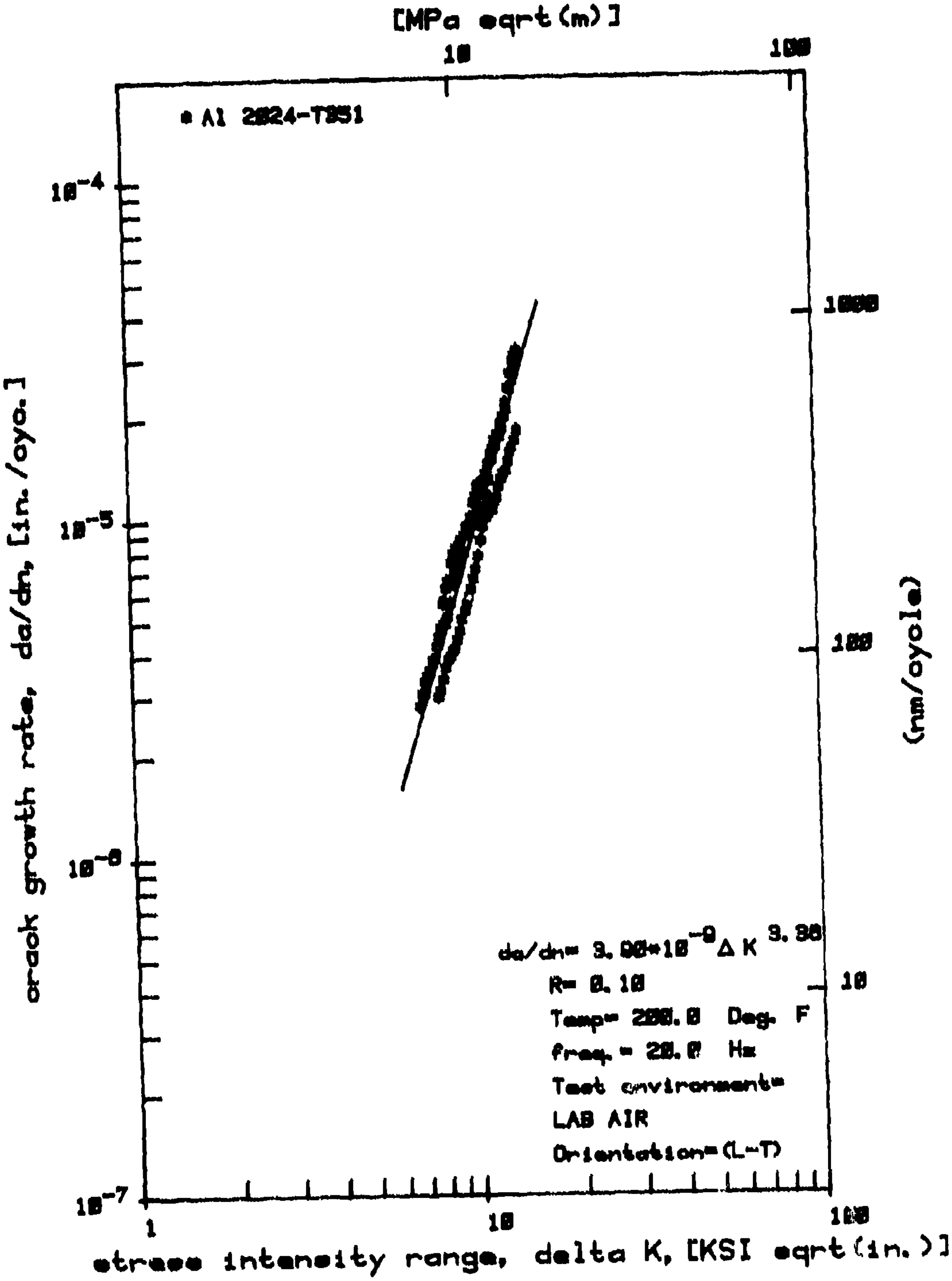

Figure A.7. R=0.1, 200°F (93°C) FCGR Test Results.

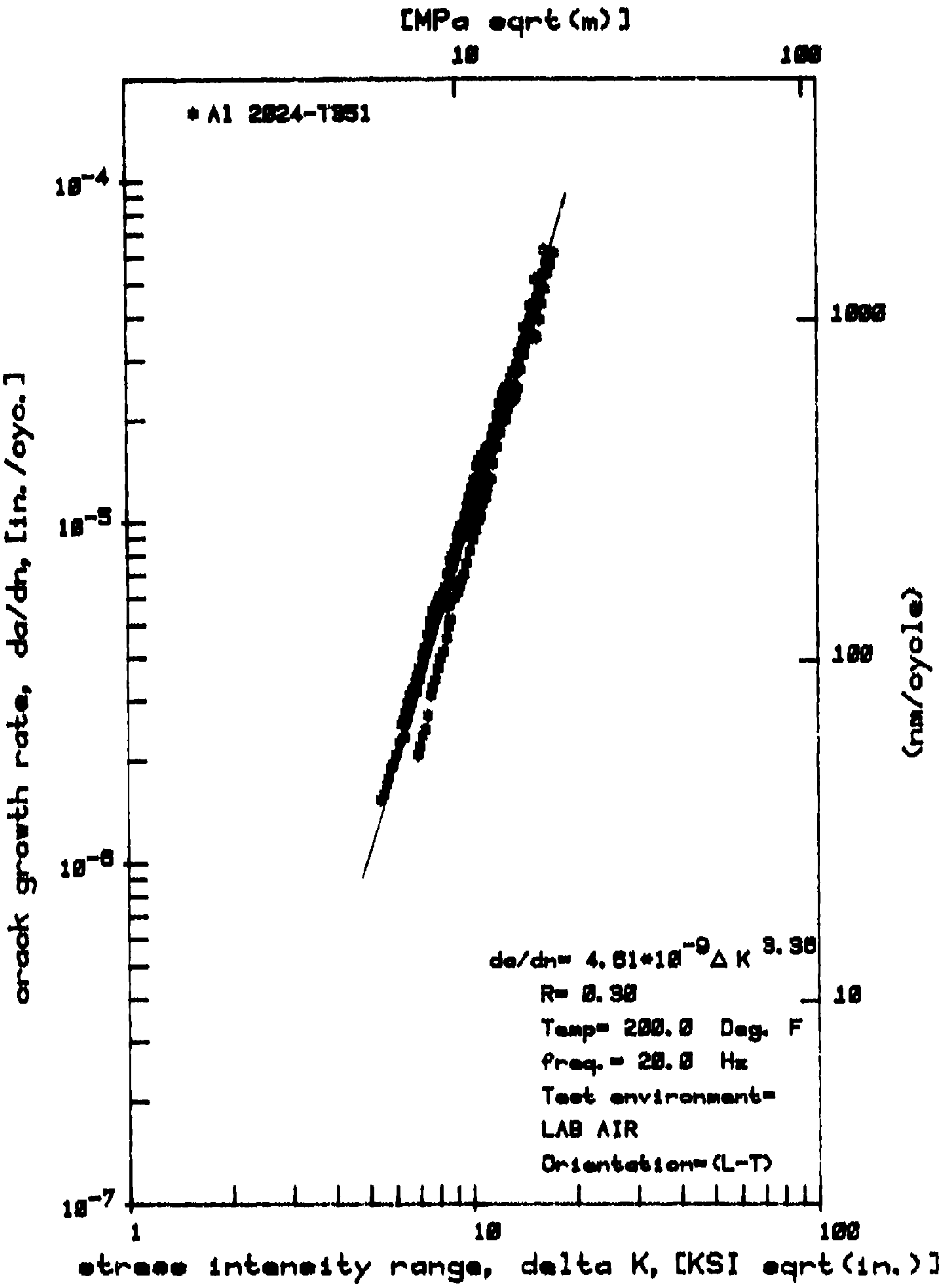

Figure A.8. R=0.3, 200°F (93°C) FCGR Test Results.

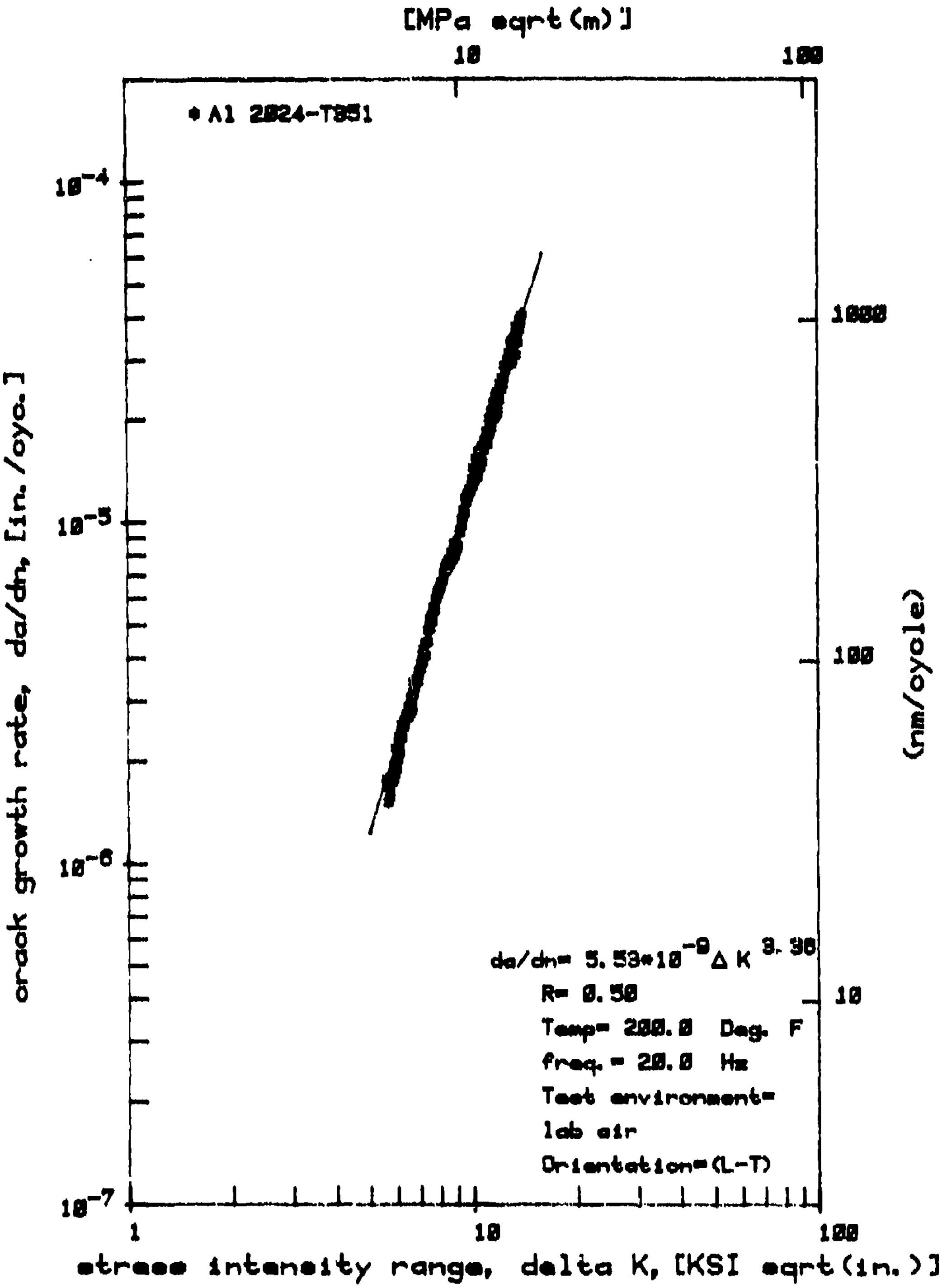

Figure A.9. R=0.5, 200°F (93°C) FCGR Test Results.

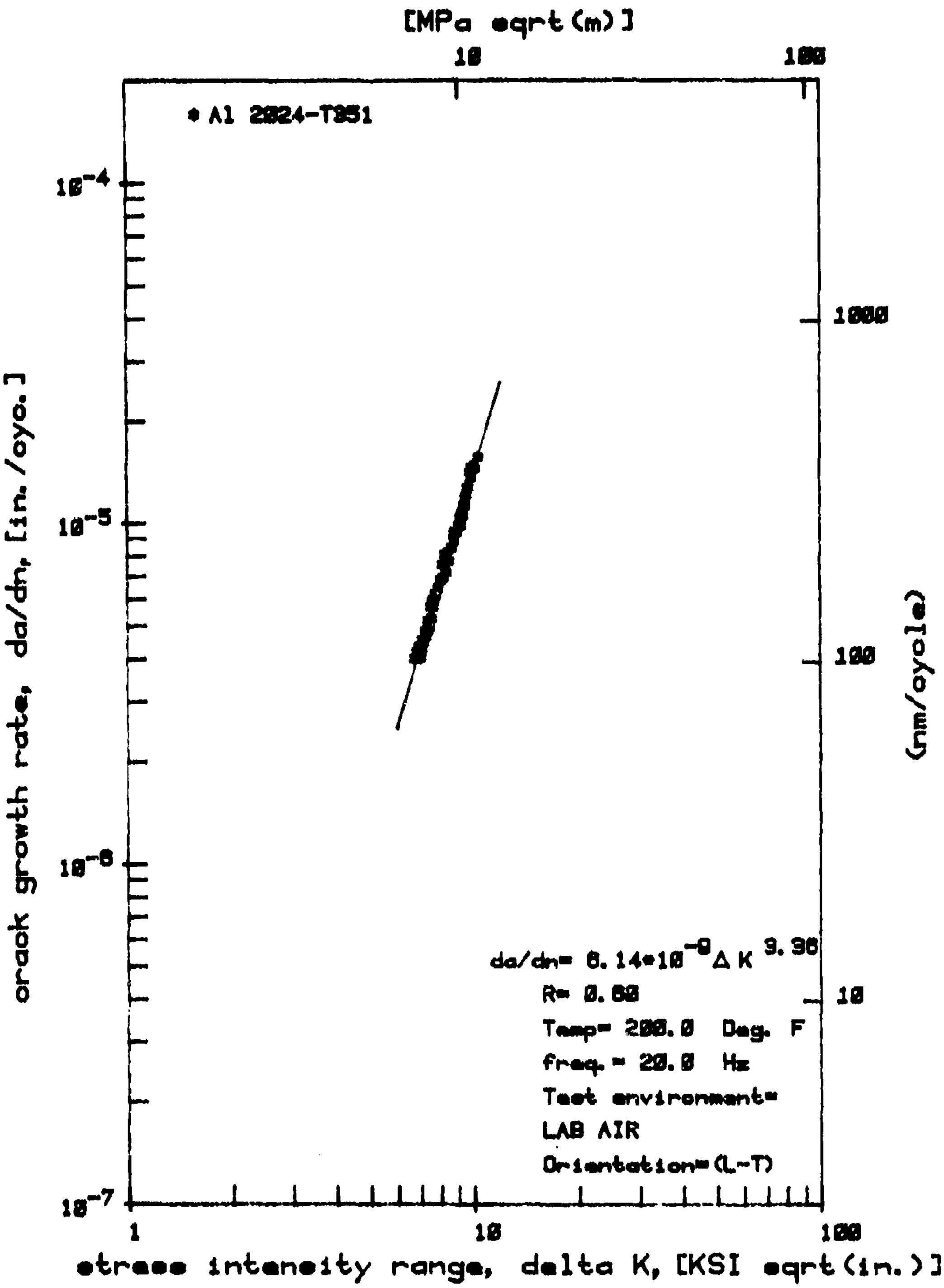

Figure A.10. R=0.6, 200°F (93°C) FCGR Test Results.

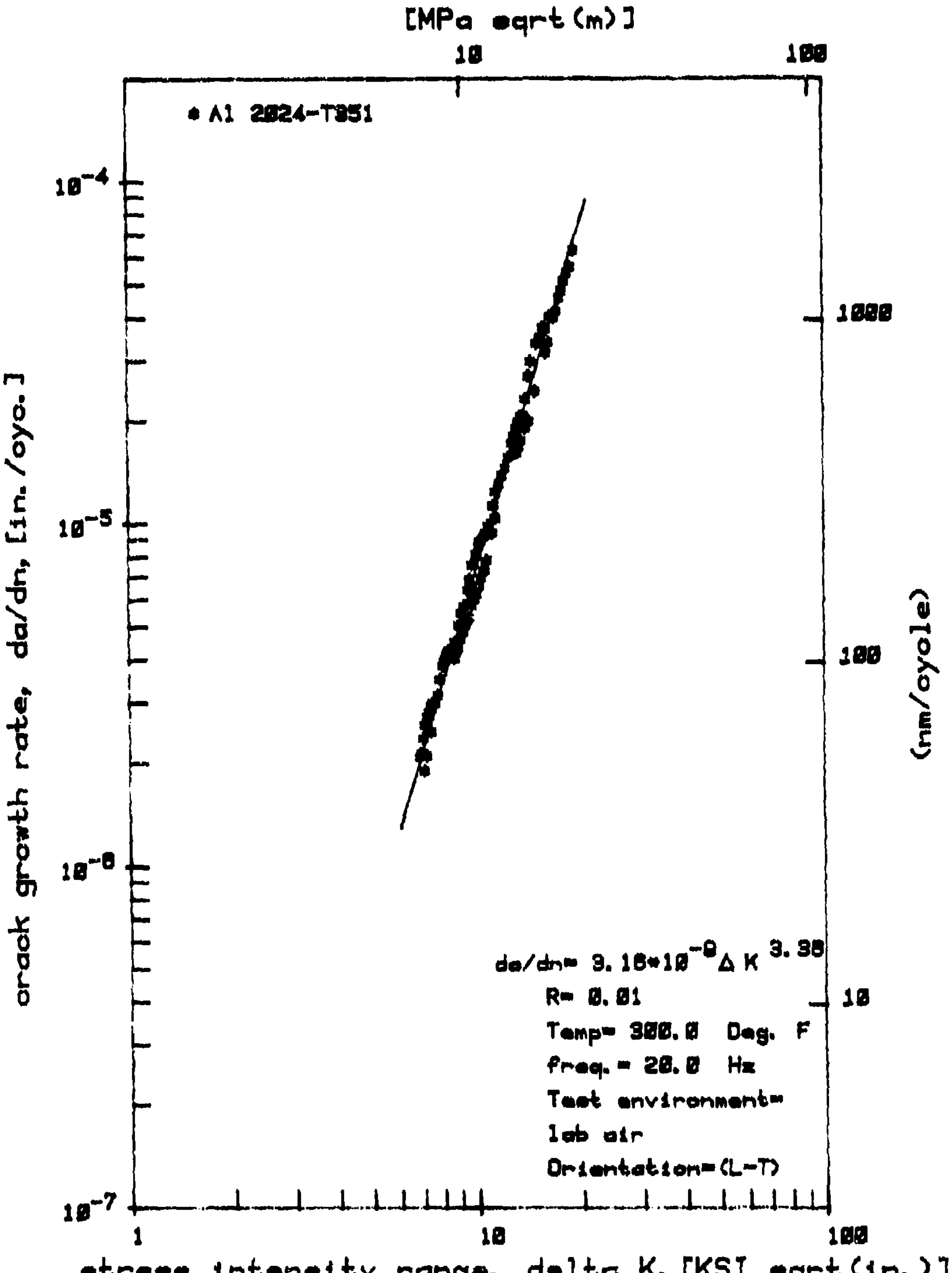

Figure A.11. R=0.01, 300°F (149°C) FCGR Test Results.

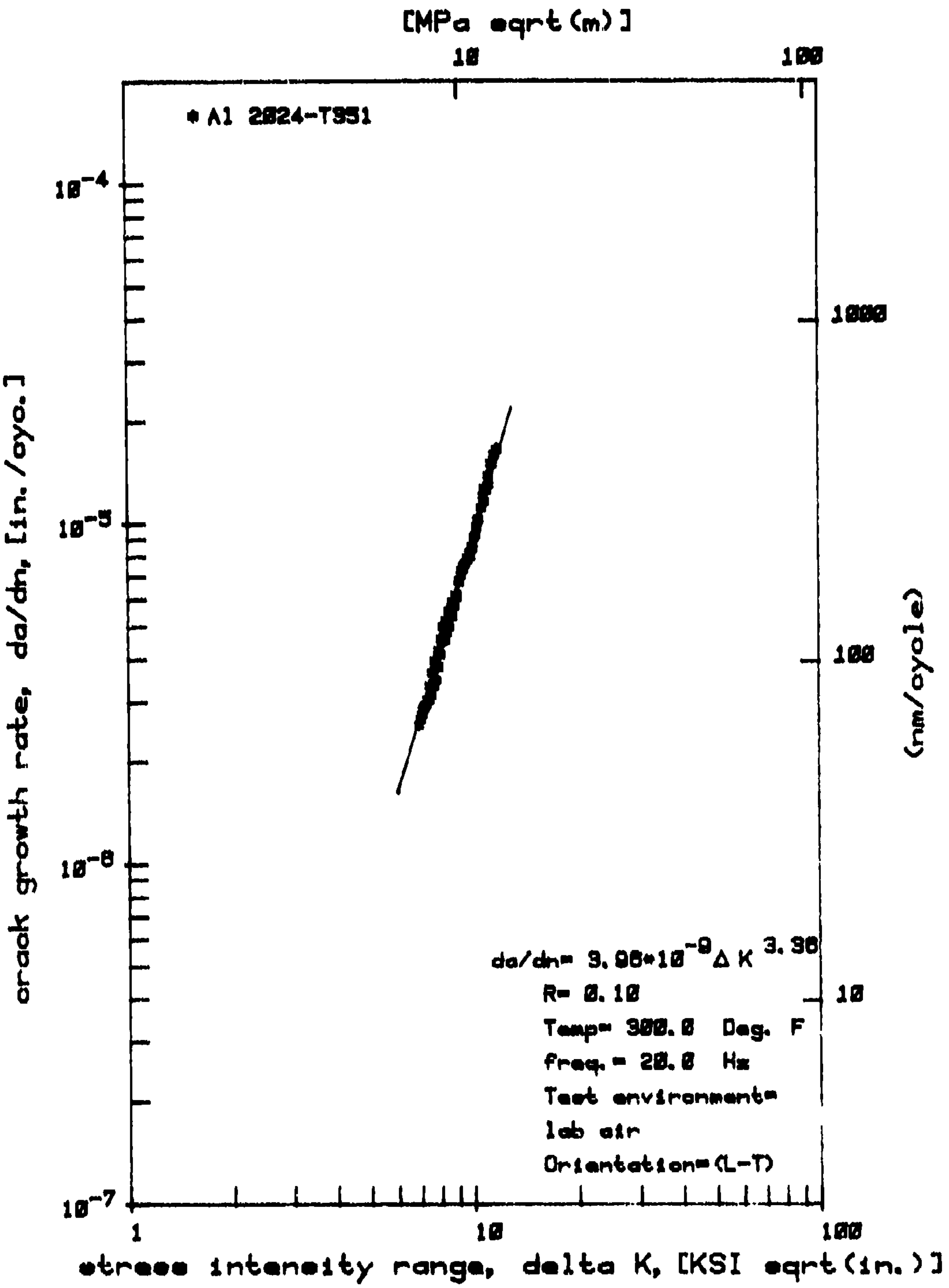

Figure A.12. R=0.1, 300°F (149°C) FCGR Test Results.

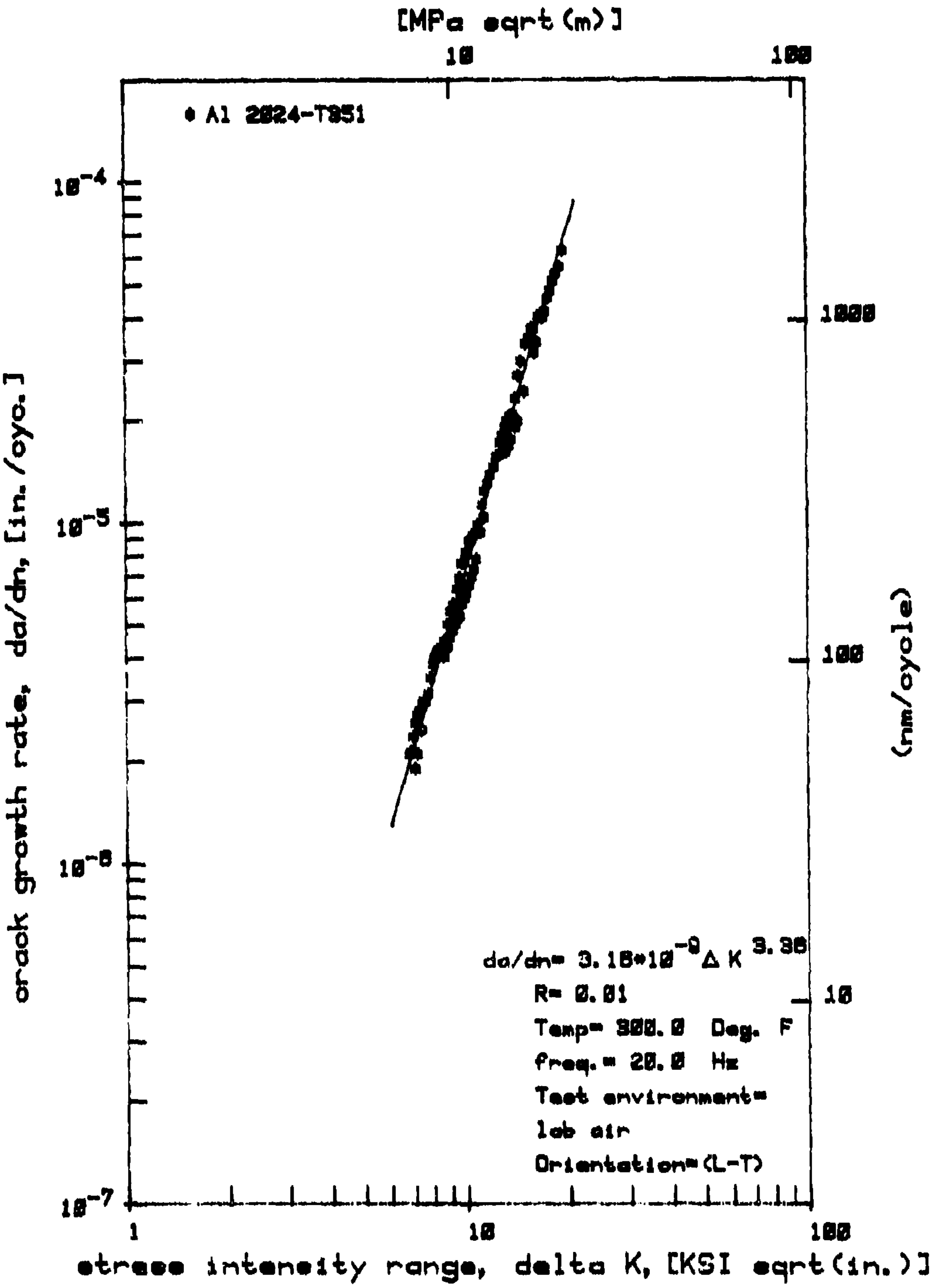

Figure A.11. R=0.01, 300°F (149°C) FCGR Test Results.

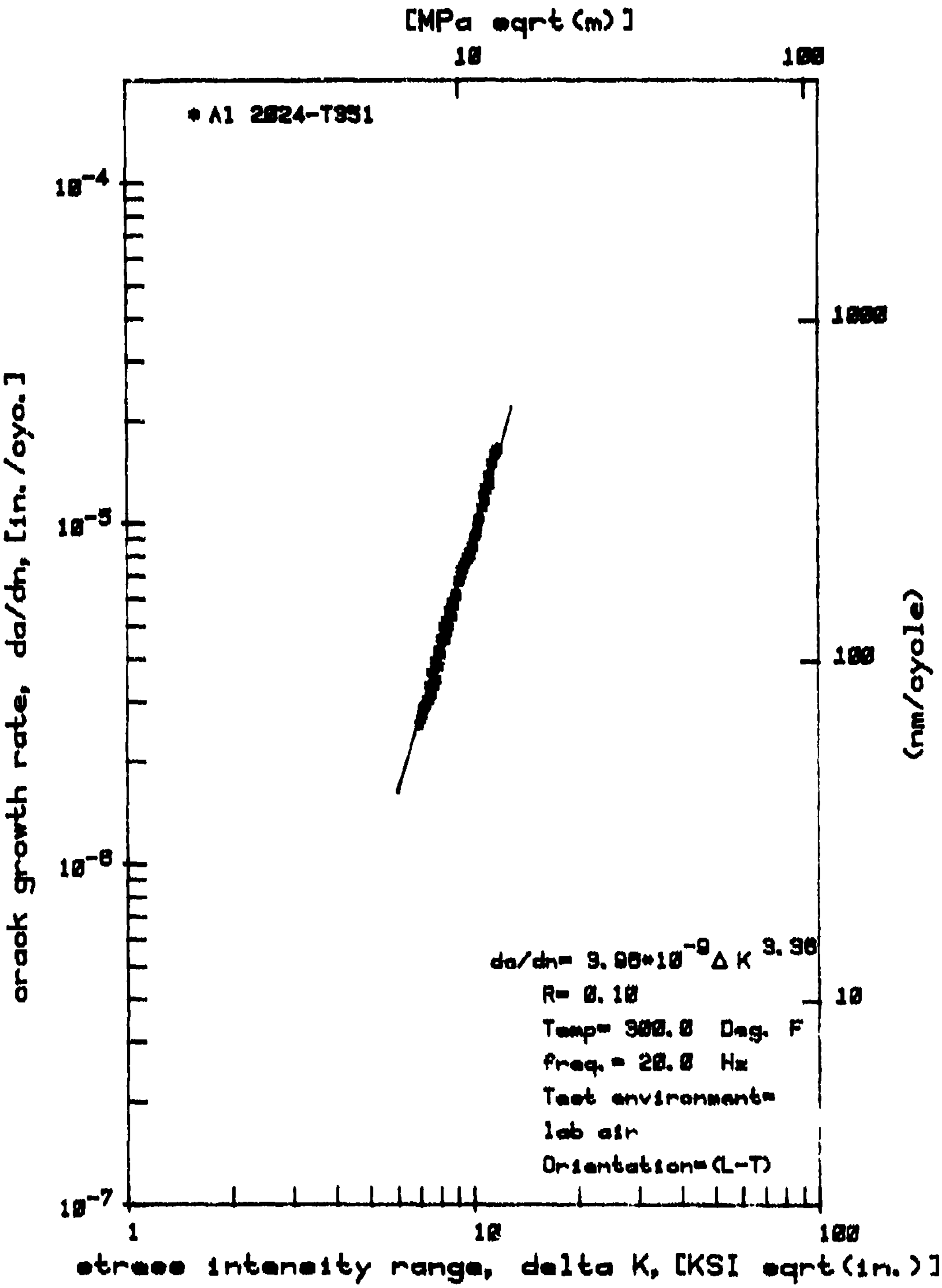

Figure A.12. R=0.1, 300°F (149°C) FCGR Test Results.

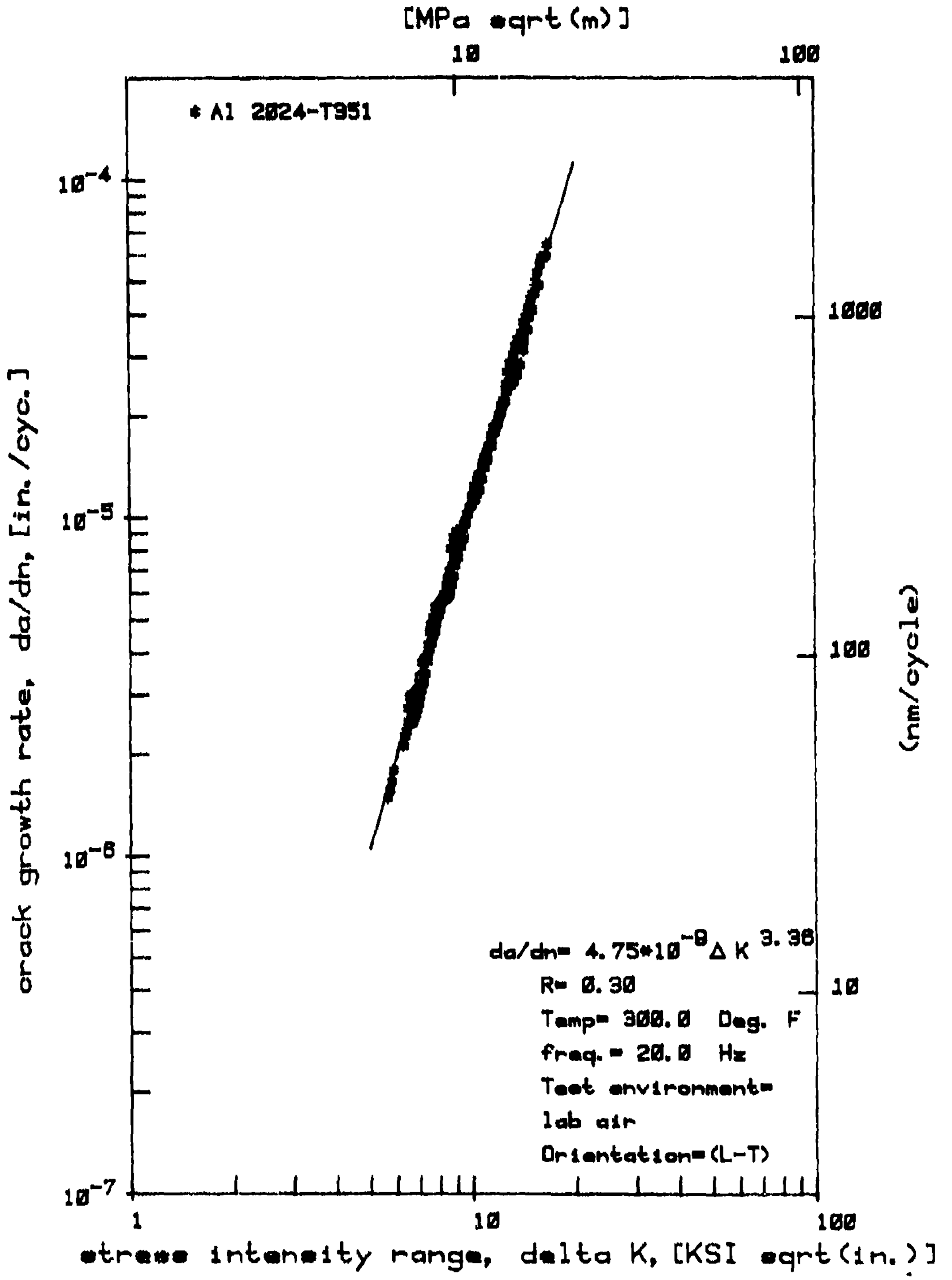

Figure A.13. R=0.3, 300°F (149°C) FCGR Test Results.

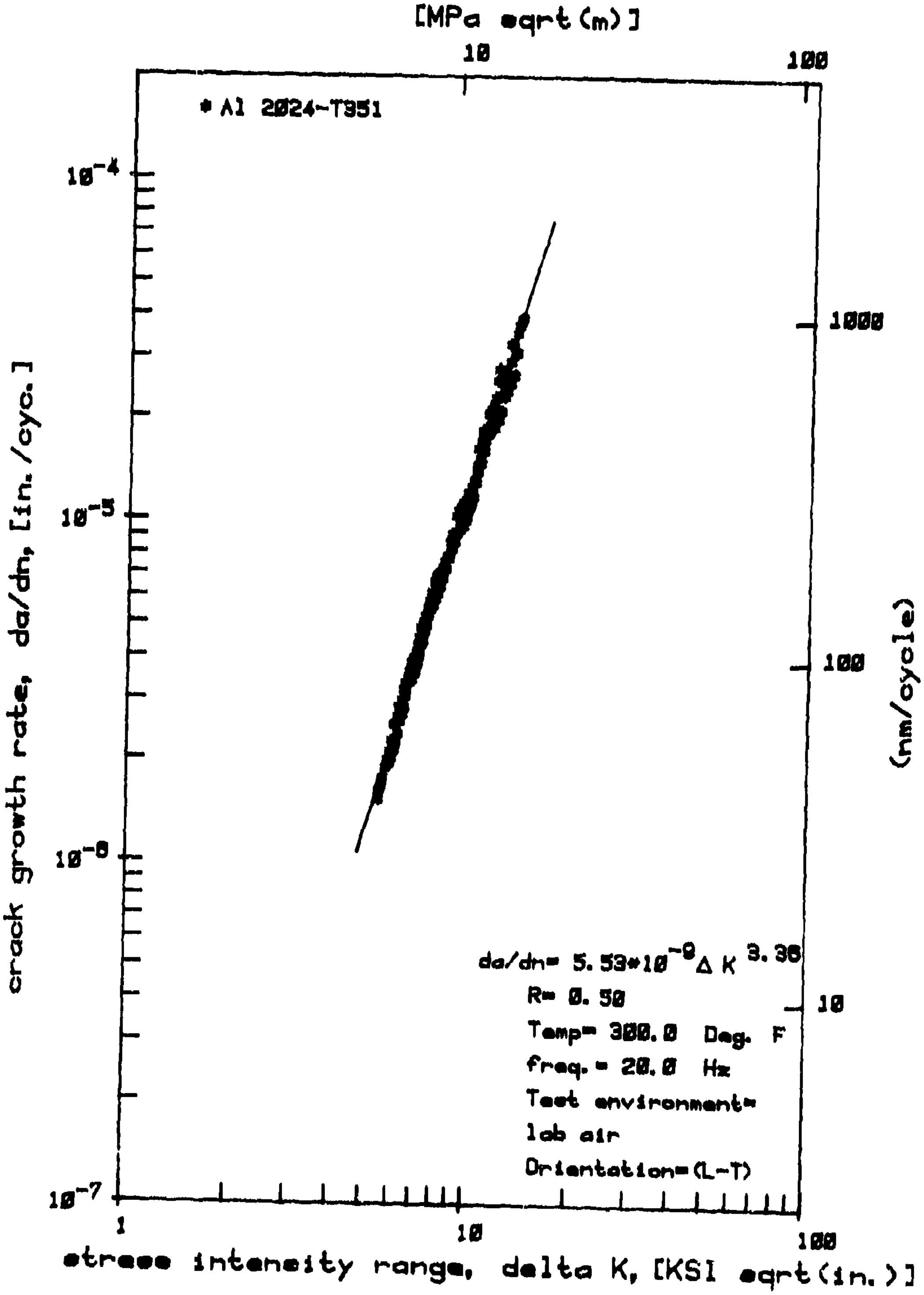

Figure A.14. R=0.5, 300°F (149°C) FCGR Test Results.

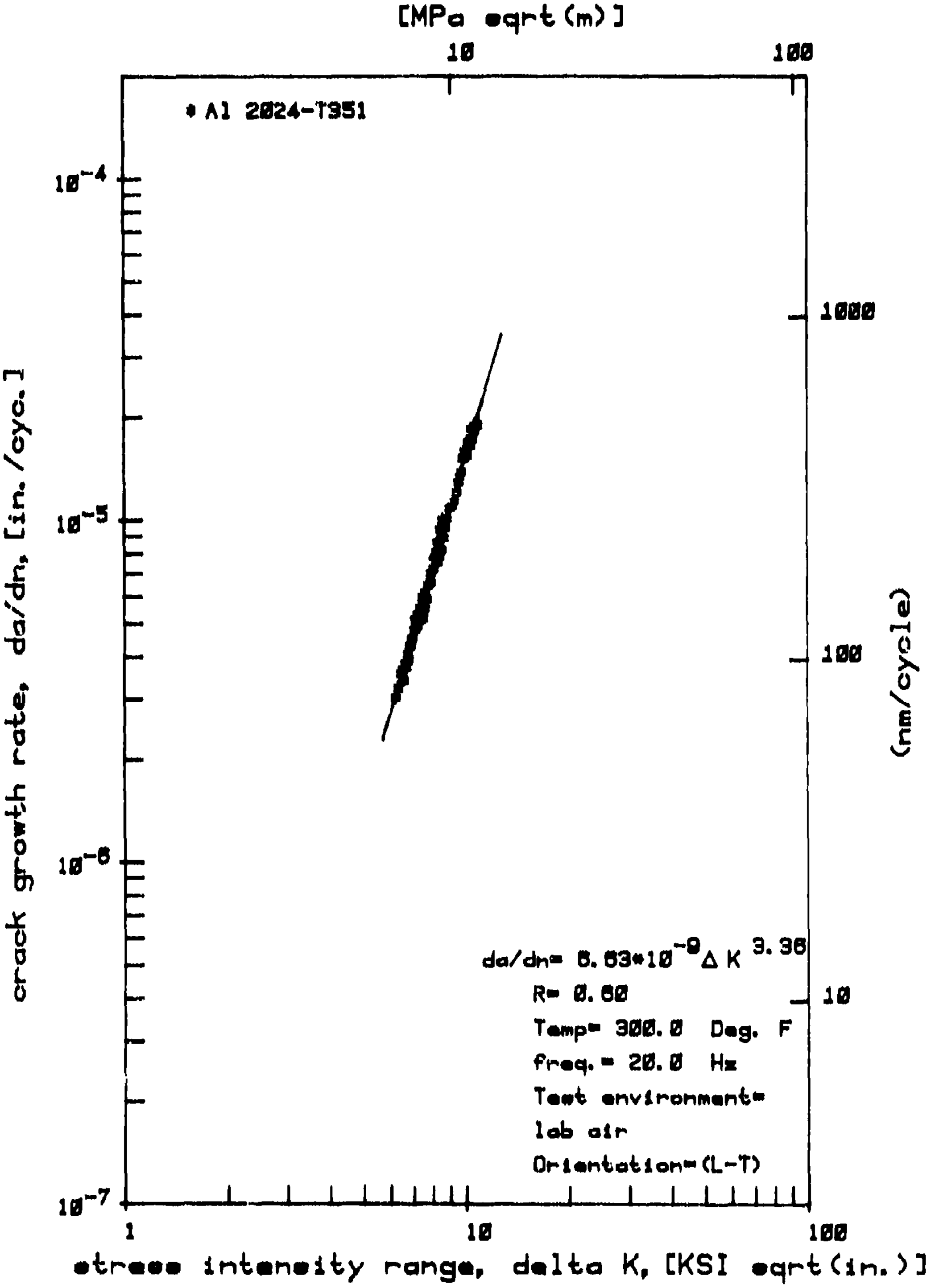

Figure A.15. R=0.6, 300°F (149°C) FCGR Test Results.

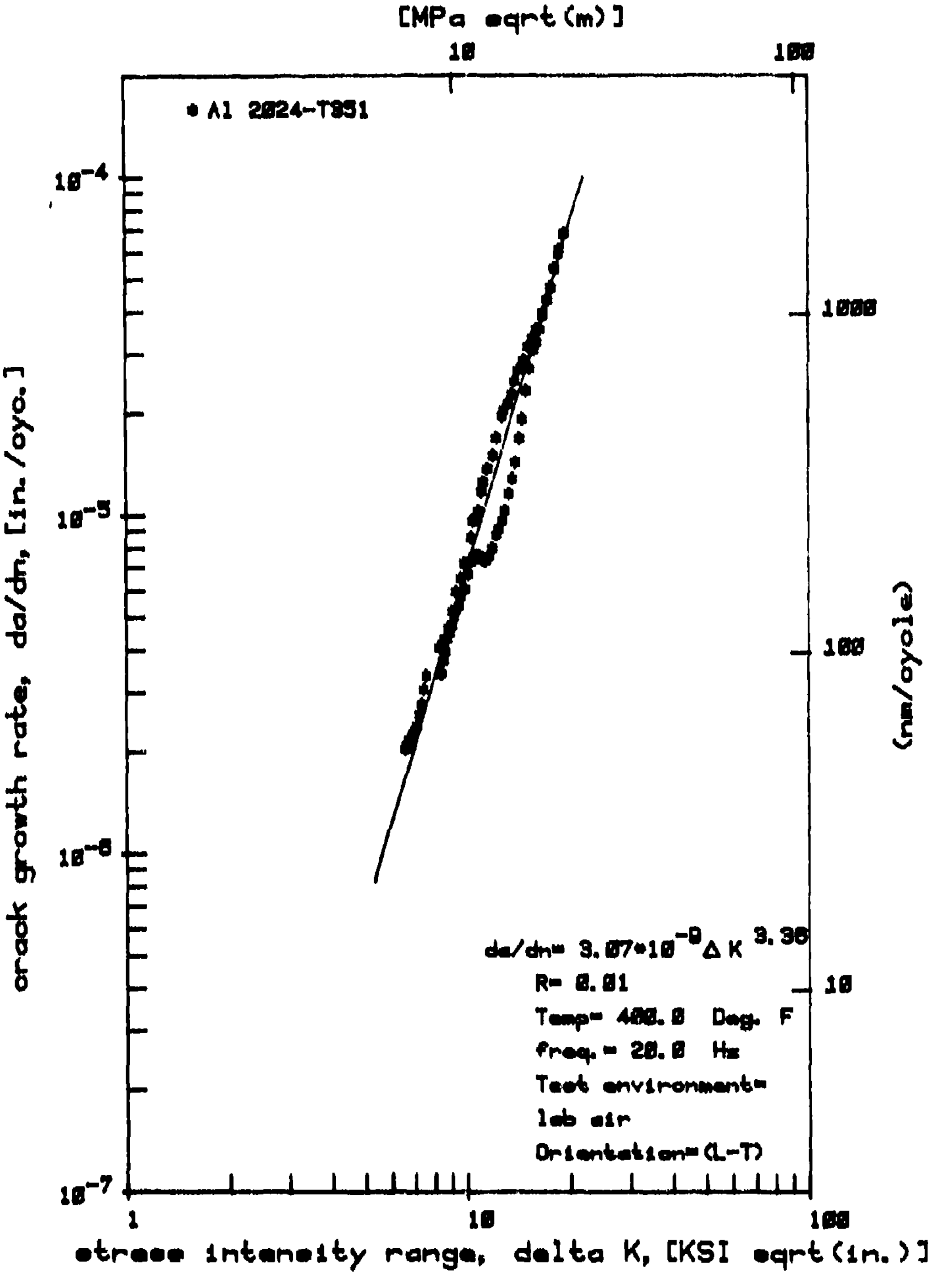

Figure A.16. R=0.01, 400°F (204°C) FCGR Test Results.

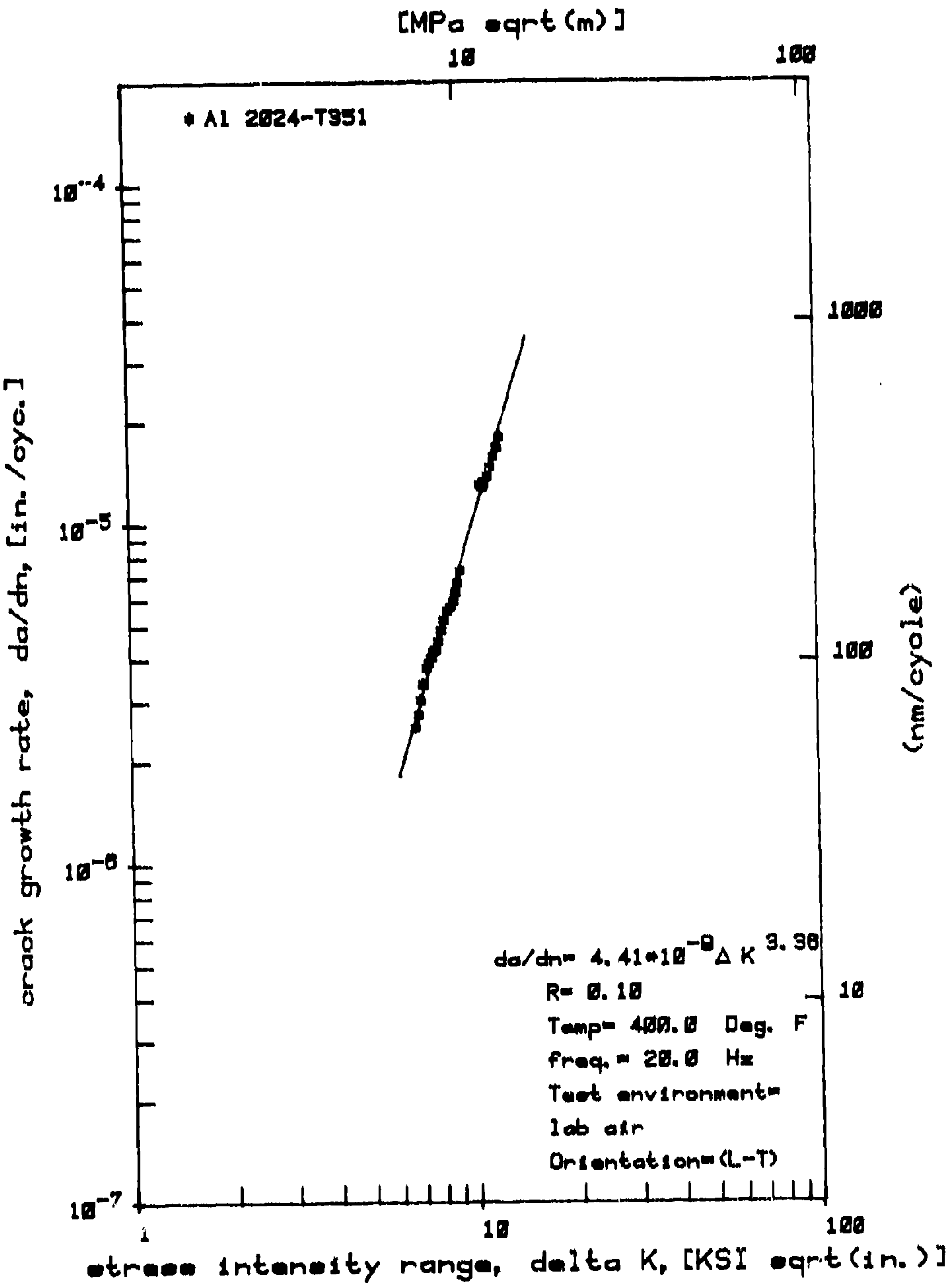

Figure A.17. R=0.1, 400°F (204°C) FCGR Test Results.

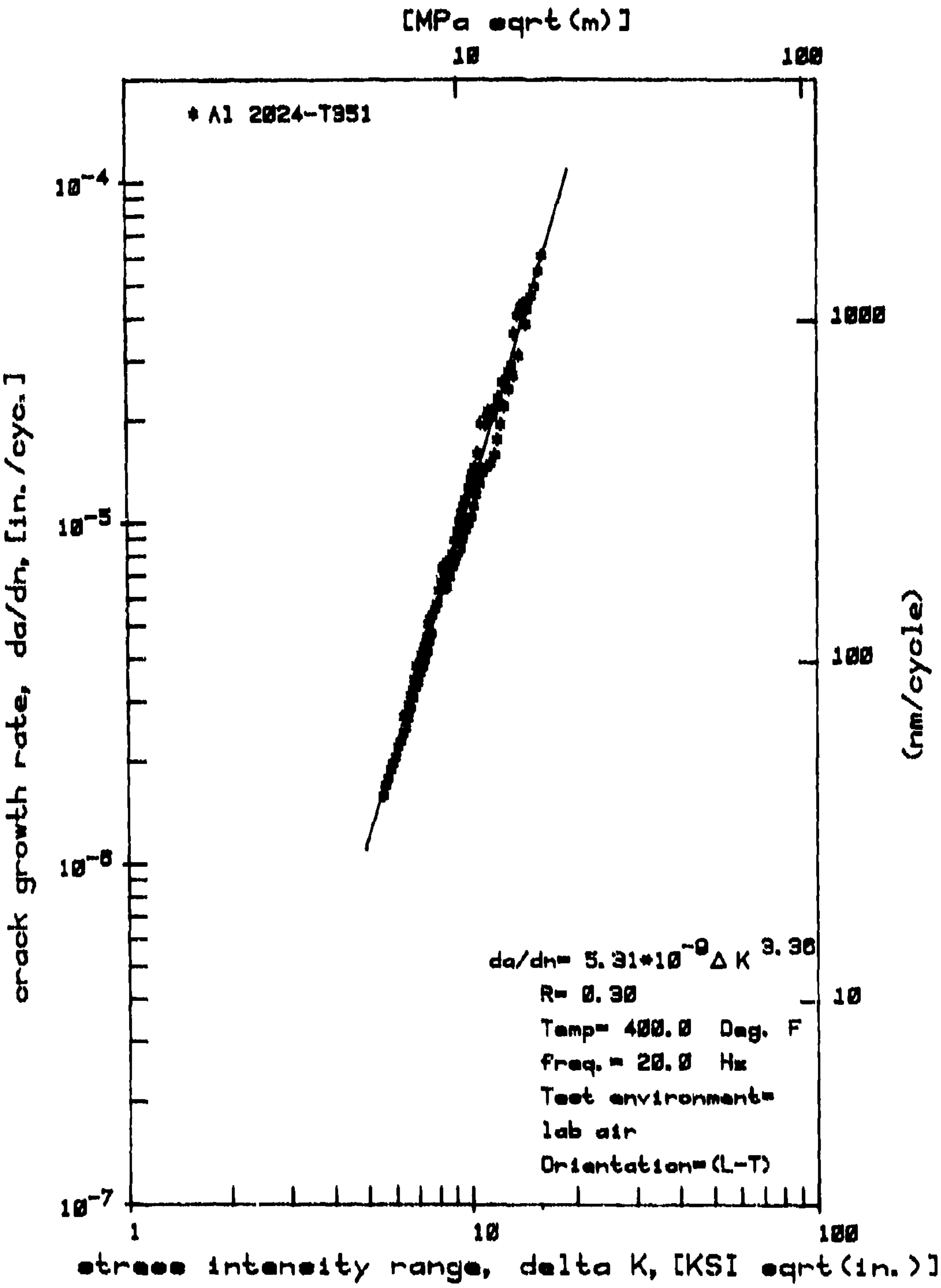

Figure A.18. R=0.3, 400°F (204°C) FCGR Test Results.

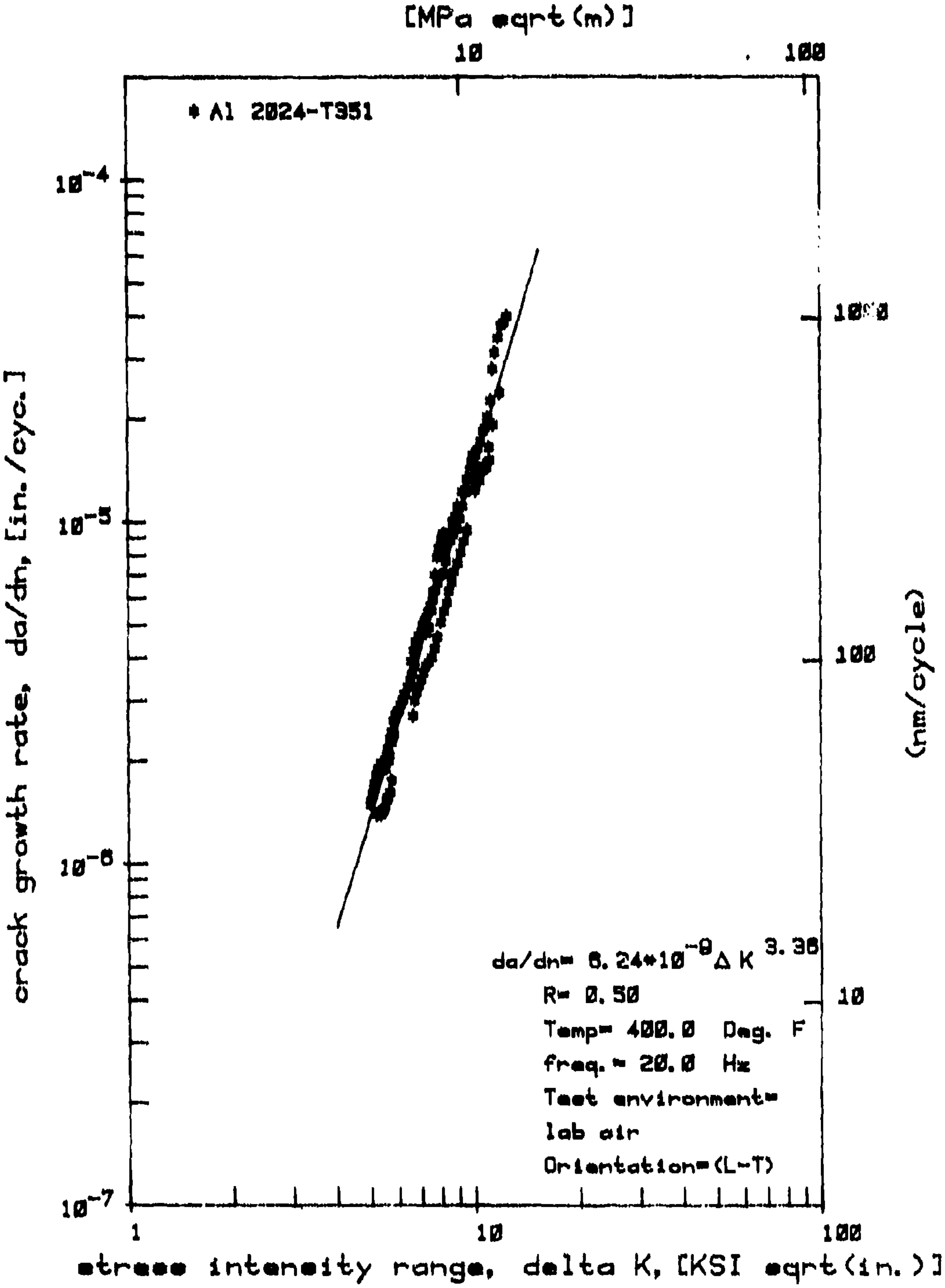

Figure A.19. R=0.5, 400°F (204°C) FCGR Test Results.

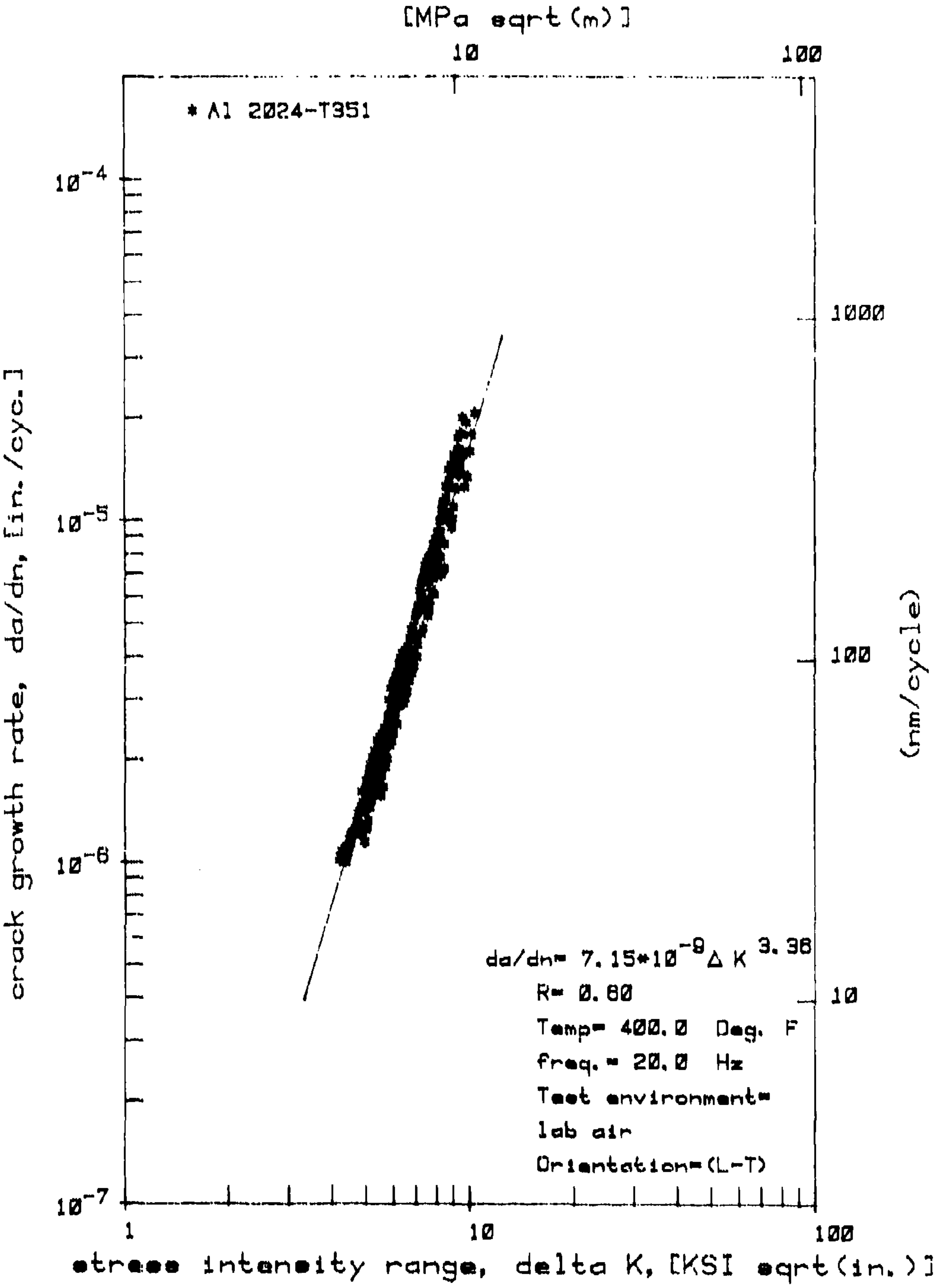

Figure A.20. R=0.6, 400°F (204°C) FCGR Test Results.